

**Middle to Late Triassic  
(Ladinian to Carnian) palynology of  
shallow stratigraphic cores 7831/2-U-2 and  
7831/2-U-1, offshore Kong Karls Land,  
Norwegian Arctic**

**Anders R. Meltveit**



**Thesis for master degree in Petroleum Geoscience**

**Department of Earth Science  
University of Bergen**

**November 2015**



## Abstract

During the Triassic, the Barents Shelf was situated on the northwestern corner of the Pangaea supercontinent as a large epicontinental seaway. Into early Late Triassic (Carnian), a major delta, prograding from the southeast towards the northwest, reached the Svalbard area. In 2005, the NPD drilled five shallow stratigraphic cores through Upper and Middle Triassic strata offshore Kong Karls Land, Svalbard. In the present study, the two oldest cores (7831/2-U-2 and 2-U-1) have been studied by applying palynology and palynofacies analyses. This contributes to the knowledge of the Triassic palynostratigraphy in the region and aids in the interpretation of the palaeoenvironment.

The lowermost core 7831/2-U-2 comprises 13.3 meter of shale, correlated to the Botneheia Formation. The palynological samples from the oldest core yielded poorly preserved palynomorphs, dominantly bisaccate pollen, algae and acritarchs. The core is assigned to the late Ladinian age *Echinitosporites iliacooides* CAz based on the occurrence of the nominate taxon, confirming the preliminary interpretation of Vigran et al. (2014). The younger core (7831/2-U-1) spans 20.95 meter of the Tschermakfjellet Formation. Palynological analysis of the core reveals an upwards increase of spores, coupled with a decrease in bisaccate pollen and marine palynomorphs. Core 7831/2-U-1 is assigned to the early Carnian *Aulisporites astigmosus* CAz based on observations of *A. astigmosus*, again confirming the age assignment of Vigran et al (2014). These age interpretations are also consistent with published Re-Os dates (Xu et al., 2014), which place the Ladinian – Carnian (Middle – Late Triassic) boundary within the upper part of the core 7831/2-U-2, and constrain the overlying core 7831/2-U-1 to the earliest Carnian.

The palynofacies analysis of this oldest core revealed a total dominance of amorphous organic matter (AOM), indicative of deposition in an anoxic environment. The palynofacies analysis of this youngest core revealed an increasing input of terrestrial organic matter. This is consistent with previous studies from the area, documenting the arrival of a prograding, early Carnian delta in the region.

The study is part of a larger industry consortium under the FORCE umbrella, where the main aim is to further enhance the resolution of the Upper Triassic Series in the Norwegian Arctic region. The present study therefore provides an important input towards this overarching goal.



## Acknowledgments

Firstly, I would like to thank my supervisor Prof. Gunn Mangerud and co-supervisor Dr. Niall W. Paterson (Department of Earth Science, University of Bergen) for all their help, support and valuable discussions.

I would also like to thank my co-supervisor Bjørn Anders Lundschien (NPD) and Prof. Ille Atle Mørk (Department of Geology and Mineral Resource Engineering, NTNU and SINTEF) for sharing their knowledge during a core viewing session.

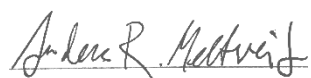
Special thanks go to Prof. G. Mangerud for raising funds enabling me to join the Boreal Triassic II Conference 2015, and to B. A. Lundschien and the NPD for inviting me to join their field excursion to Edgeøya and Hopen in August 2014.

The present study is part of a larger industry consortium under the FORCE umbrella, with the contributing companies:

A/S Norske Shell, Centrica Energi NUF, Chevron Norge AS, ConocoPhillips Skandinavia AS, Det Norske Oljeselskap ASA, Dong E&P Norge AS, ENI Norge AS, Lundin Norway AS and Statoil Petroleum AS. Thank you for financing this project.

I would also like to thank Dr. Stijn De Schepper (Department of Earth Science, University of Bergen) for his lectures about dinoflagellates and palynological processing techniques.

Lastly, I wish to thank my parents and sister for their kind interest in my studies and all their support.



Anders Røsgård Meltveit

Bergen, November 16, 2015



## Table of contents

<b>1. Introduction</b> .....	1
1.1 Aim of study .....	3
1.2 Palynology .....	4
1.3 Previous palynological work .....	6
<b>2. Geological setting and lithostratigraphy</b> .....	9
2.1 The Barents Sea area .....	9
2.2 The Barents Sea area during the Triassic .....	10
2.3 The Triassic lithostratigraphy of Svalbard and the Barents Sea area .....	13
<b>3. Materials and methods</b> .....	15
3.1 Collection of material .....	15
3.2 Palynological preparation .....	17
3.3 Microscopy and palynological analyses .....	17
3.4 Palynofacies .....	19
<b>4. Results</b> .....	23
4.1 Quantitative palynology .....	23
4.1.1 Core 7831/2-U-2 (Botneheia Formation) .....	23
4.1.2 Core 7831/2-U-1 (Tschermakfjellet Formation) .....	26
4.2 Core description .....	29
4.2.1 Core 7831/2-U-2 (Botneheia Formation) .....	29
4.2.2 Core 7831/2-U-1 (Tschermakfjellet Formation) .....	35
4.3 Palynofacies analysis .....	39
4.3.1 Core 7831/2-U-2 (Botneheia Formation) .....	40
4.3.2 Core 7831/2-U-1 (Tschermakfjellet Formation) .....	41

<b>5. Discussion</b> .....	43
5.1 Palynostratigraphy and age determination .....	43
5.2 Palaeoenvironment .....	53
<b>6. Conclusions</b> .....	57
<b>References</b> .....	59
<b>Appendices</b> .....	63
Appendix I: List of palynomorph taxa .....	63
Appendix II: Table of Re-Os datings from cores 7831/2-U-2 and 7831/2-U-1 .....	68
Appendix III: Range charts .....	69
Appendix IV: Plates .....	70



## 1. Introduction

This study concerns the palynology of two shallow stratigraphic cores, spanning the Ladinian - Carnian (Middle – Late Triassic) transition (Fig. 1), drilled offshore Kong Karls Land, Svalbard (Figs. 2, 4 and 8). In this area, the Jurassic succession is strongly glacially eroded and thus often thin or absent. This makes the Triassic System especially important for the petroleum industry in order to understand the petroleum play in the region (Lundschieen et al., 2014). Because of this erosion, the Triassic System is outcropping over large areas (Riis et al., 2008, Fig. 2). This geological setting allows use of shallow stratigraphic drilling to obtain cores with a good coverage of the Triassic successions (Riis et al., 2008, Fig.5). Core 7831/2-U-2 has previously been correlated to the Botneheia Formation (Riis et al., 2008), whereas core 7831/2-U-1 comprises rocks of the Tschermakfjellet Formation (Riis et al., 2008). Xu et al. (2014) have recently performed Re-Os datings of the two cores, constraining the Ladinian – Carnian boundary within the two cores (Appendices II and III). The Triassic Period spans 50.9 million years, with the Late Triassic being the longest epoch. The durations of the Middle and Late Triassic are 10.1 and 35.7 million years, respectively (Fig. 1). Ammonites and conodonts are best suited for subdivision of the Boreal Triassic, but their overall scarcity in the region, cause difficulties regarding confident correlation to the zonations in the Germanic and Alpine realms (Hochuli et al., 1989). Because of this, there are some major uncertainties, especially regarding the chronostratigraphic subdivision of the Ladinian, in the Boreal realm (Hochuli et al. (1989). This makes palynology an essential tool in order to improve the Triassic resolution in the region. The Boreal Triassic palynomorph associations are mainly of marine character, but with major input of terrestrial sporomorphs (Vigran et al., 2014). This limits confident correlation to the palynozonations of the Tethyan and Germanic realms, as these palynofloras are mainly of non-marine character (Hochuli et al., 1989). In addition, there seems to be palaeoclimatic differences between the Germanic, Tethyan and Boreal realms, causing differences in the assemblages (Hochuli et al., 1989; Hochuli et al., 2014). Vigran et al. (2014) applied palynology to divide the Middle and Late Triassic into four zones, respectively (Fig. 1). This gives the zones an average duration of 2.55 and 8.90 million years, respectively. Thus, further biostratigraphic work is important, especially for the Late Triassic.



## 1.1 Aim of study

The main aim of this study was to make an attempt to define the Ladinian – Carnian boundary based on palynological criteria. Since Re-Os dating was available, the data set provided a unique opportunity to explore whether palynology alone can be used for this purpose. The study therefore comprised detailed semi-quantitative studies of the shallow stratigraphic cores 7831/2-U-2 and 7831/2-U-1, trying to outline the palynological differences between the two.

A secondary goal of this thesis was to integrate sedimentological and palynofacies analyses to interpret the palaeoenvironment. The semi-quantitative palynological analysis was combined with sedimentological analysis, although the latter only was based on a relatively brief sedimentological description due to time constraints within the time frame of a master thesis.

Comparison and correlation of the cores in relation to core 7534/4-U-1 from the Sentralbanken High area, have also been carried out. This latter, initially thought to represent the same stratigraphic interval, has been analysed by another master student at the University of Bergen (Landa, 2015).

The study is part of a larger industry consortium under the FORCE umbrella, where the main aim is to further enhance the resolution of the Upper Triassic Series in the Norwegian Arctic region by applying palynology. The present study therefore provides an important input to this overarching study in order to improve our understanding of the Upper Triassic development.

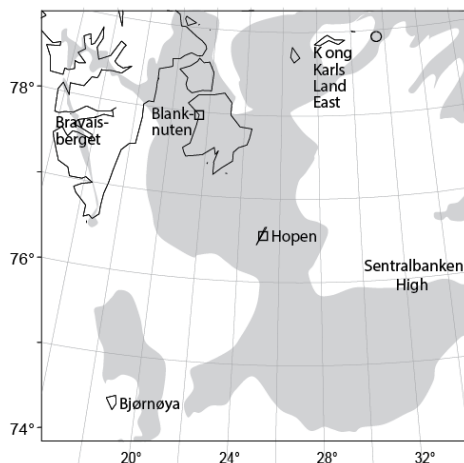


**Figure 2:** Location of the shallow stratigraphic cores east of Kong Karls Land. Gray shading indicates Triassic rocks outcropping onshore and offshore. (modified from Riis et al., 2008).

## 1.2 Palynology

Palaeopalynology (called palynology herein) is the science dealing with palynomorphs, a collective term for pollen, spores, acritarchs, dinoflagellate cysts, scolecodonts, chitinozoans, and certain algal and fungal dispersal bodies (Traverse, 2007). Tschudy (1961) introduced the term, referring to all organic-walled (unicellular, multicellular or colonial) microfossils that can endure palynological maceration, in other words are acid-resistant.

Palynology as a science originated from the quaternary pollen analyses, and the year 1916 is commonly considered as the time of establishment. This happened with the publication of the first modern percentage pollen diagram (Mantel, 1967). Even though the science had existed for some time, Hyde and Williams (1944) first introduced the term "palynology". They defined it as *"the study of pollen and other spores and their dispersal, and applications thereof"*. Their new term was readily accepted by the scientific society, but their initial definition of the word has changed throughout time and is now redefined to also include other microscopic fossils.

Palynomorphs are classified based on their morphology, and their classification is thus artificial (Traverse, 2007) causing that no natural affinity is required within each subdivision. Spores and pollen, collectively termed sporomorphs, are produced during the life cycle of land plants. Spores are unicellular, reproductive units, produced in tetrads by bryophytes (e.g. mosses), pteridophytes (ferns) and their primitive precursors (Traverse, 2007). They are often round to subtriangular in shape, often with a trilete mark. This is a "Y" shaped "scar" resulting from when the spores made up tetrads. Monolete ("I" shaped) marks also occur, but are less common (Armstrong and Brasier, 2005). Spores can be of different sizes, shapes and have different ornamentations (verrucate, baculate, etc.) (Fig. 10). Pollen is produced by land plants such as gymnosperms (e.g. conifers and ginkgos) and angiosperms. Acritarchs (Fig. 3) are single celled, organic walled microfossils of unknown affinity. Most are probably of marine algal origin (Traverse, 2007). Early forms of possible planktonic affinity have been recorded from Precambrian strata three billion years old (Downie, 1967).

In terms of size it is generally agreed, is that palynomorphs range within 5 to 500 micrometers in size (Traverse, 2007), although they commonly range from 20 to 60 micrometers, which is within the silt fraction. Thus, palynomorphs are mostly found in clay- and siltstones. Hoffmeister (1954) stated that the distribution of sporomorphs in sediments follows sedimentological principles in essence. Because of this, the abundance of spores and pollen decrease markedly, approximately logarithmically, seawards (Abbink, 1998). Several authors have used this approach, especially has the method on Sporomorph Eco Groups (SEGs) established by Abbink (1998) been widely used.

Palynology is a science of diverse applications, and is thus used in a variety of fields, which partly applies different techniques. This makes it a challenge to establish a concise terminology and a common standardized technique for the various processes, which includes the sampling, preparation, analyses and presenting of results. Several publications have been published to simplify the application of palynological terms and to make it more accessible (e.g. Punt et al., 2007). Palynology offers many advantages. Palynomorphs are distributed in large numbers, over vast areas, and are the only fossil group that can be used in correlation between terrestrial and marine strata (Traverse, 2007). They are embedded within sediments and sedimentary rocks, making them relatively easy to find and sample. A small sample, about 30 grams, is also all that is needed to make the preparations. Palynomorphs show a rapid evolutionary development, as reflected by their high diversity. This makes them suitable for dating of the sedimentary rock record. Due to the composition of their wall, which consists mainly of sporopollenin or chitin, they have excellent preservation potential. These organic compounds are probably the most chemically inert that exist and palynomorphs are thus highly resistant to most forms of decay, except oxidation (Traverse, 2007).

Palynological dating and correlation are normally carried out by defining different types of palynostratigraphic zones in preferentially independently dated by for example ammonites. Recognition of these palynozones elsewhere can then be used to date strata where age-diagnostic macrofossils are absent. Formal definition of biostratigraphic zones follows official nomenclatures. In Norway most workers follow Nystuen (1989). Palynological assemblage zones are often named after diagnostic pollen species, but spores (e.g. Paterson and

Mangerud, 2015), dinoflagellates (e.g. Vigran et al., 2014) and acritarchs (e.g. Raevskaya and Servais, 2009) have also been used successfully to define zones.

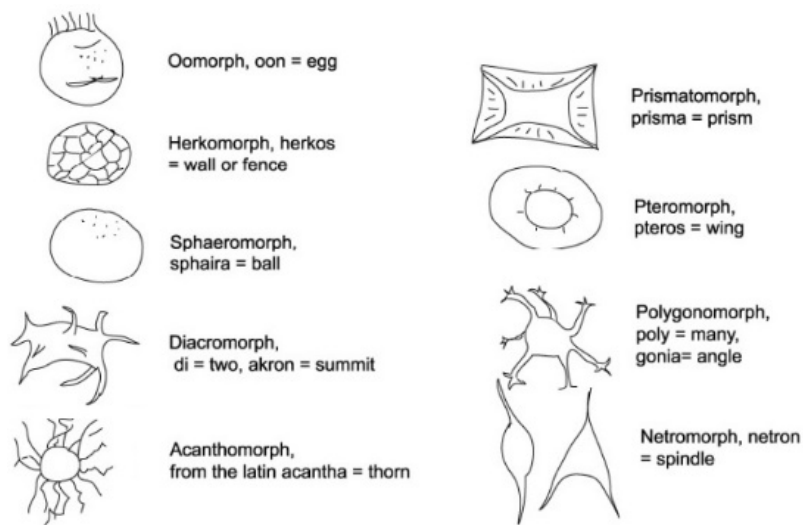


**Figure 3:** Classification of acritarchs into nine groups based on their morphology (figure from: [www.ucl.ac.uk/GeolSci/micropal/acritarch.html](http://www.ucl.ac.uk/GeolSci/micropal/acritarch.html))

### 1.3 Previous palynological work

Triassic palynology has been extensively studied, especially the palynoflora of the Germanic and Alpine realms, which is well documented by numerous authors. Visscher and Brugman (1981) critically assessed 52 palynomorph species or genera, from Alpine Triassic regions of Germany, Austria, Italy, Hungary and Yugoslavia. No formal scheme was established, but their work yielded five palynostratigraphic range charts, including one for the Ladinian and another spanning the Carnian. Palynological data supported by independent ammonite datings was especially emphasized. Van der Eem (1983) carried out an extensive investigation into the Middle and Late Triassic palynology in the western Dolomites, in the type sections of the Ladinian and the early Carnian. Seven characteristic “palynological phases” were introduced based on their assemblages. Three of which spanning the Ladinian - Carnian transition, and controlled by ammonites. Several taxa and combinations were formally described for the first time. Cirilli (2010) correlated the established palynozonations of the Late Triassic to the Early Jurassic in the northern and southern hemispheres. She discussed assemblages of the Boreal

realm and pointed out the issues regarding global palynostratigraphical correlations. Kürschner and Herngreen (2010) reviewed Triassic palynofloral trends of the Alpine and Germanic realms and the palynozonations of these regions. The pioneering work of Mädler (1964), earned him his doctoral degree from the Technical University of Hannover. In his thesis, Triassic spores and pollen from Germany were studied. Mädler (1963) also showed the importance of studying plankton. Klaus (1960) studied Carnian palynomorphs from the Alpine realm in detail, and described many stratigraphic important species for the first time. Blendinger (1988) analysed palynological samples of late Ladinian to Carnian age from the Dolomites. The correlation of these samples yielded a more precise dating in the region.

Felix (1975) carried out palynological investigations on Ellef Ringnes Island, Arctic Canada, proving previously considered sediments of Jurassic age to be of possible Late Triassic age. Fisher (1979) established a palynostratigraphic zonation for the entire Triassic, by recording nine distinct palynofloral assemblages based on greatly diverse taxa from the Triassic formations of the Canadian Arctic Archipelago.

The earliest conducted Triassic palynological studies of the Svalbard archipelago (Smith, 1974; Smith et al., 1975; Bjærke and Manum, 1977; Smith, 1982) focused mainly on the Kapp Toscana Group on the Island of Hopen, the most southeastern part of the archipelago. In recent times, more detailed palynological studies of Hopen have been performed (Ask, 2013; Holen, 2014; Paterson et al. (2015). Bjærke (1977) investigated the palynology of the Mesozoic succession onshore Kong Karls Land. On the basis of this study, six palynological associations were described, ranging from Late Triassic to Early Cretaceous in age. Hochuli et al. (1989) established an informal palynostratigraphic framework for the Triassic succession in the western Barents Sea. They introduced 16 assemblages based largely on downhole first and last occurrences and abundances from cuttings samples from exploration wells, and on samples from outcrops in Spitsbergen, on Bjørnøya and from shallow stratigraphic cores. Their study presented the general features of their palynofloral assemblages, and highlighted differences from the Germanic and Alpine realms. The Early and Middle Triassic assemblages were recorded from ammonite-dated beds, thereby providing independent datings. Conodonts were also found in associations with the Early and Middle Triassic sequences, allowing correlation with the standard conodont zonation. The Late Triassic assemblages were

dated on the basis of known palynofloral ranges in the Germanic and Alpine realms. Mørk et al. (1990) applied palynology and macrofossils to perform datings of the Triassic succession on Bjørnøya. They recognized equivalent assemblages to those recorded by Hochuli et al. (1989) and correlated the succession according to these. Vigran et al. (1998) established eight assemblage zones (Svalis-1 to Svalis-8) based on Early and Middle Triassic palynomorphs from shallow stratigraphic cores from near the Svalis Dome, central Barents Sea. They calibrated six of the zones to chronostratigraphy using ammonoids from the cores. This was performed by studying samples from shallow stratigraphic cores from near the Svalis Dome, central Barents Sea. Palynofacies analyses was also conducted. Their Ladinian Svalis-8 zone, represents the Snadd Formation. This assemblage zone was further divided into three parts based on diagnostic species or relative abundances of spores and pollen. They correlated this zone to the Ladinian age I assemblage of Hochuli et al. (1989). Vigran et al. (2014) published a comprehensive book about the palynology and geology of the Triassic succession on Svalbard and the Barents Sea. This compilation of almost 40 years of research, contains palynological results of numerous samples throughout the area. Based on this work, a regional stratigraphic framework of 15 composite assemblage zones was formally established for the first time (Fig. 1). This framework serves as a solid correlation tool for the Norwegian Barents Sea. Four zones were established for the Middle and Late Triassic, respectively (Fig. 1). The *Echinosporites iliacooides* Composite Assemblage zone (CAz) was assigned to the Ladinian, spanning approximately five million years. Whereas the *Aulisporites astigmaticus* CAz was assigned to the early-mid Carnian. In the Spitsbergen area, Mueller et al. (2014) were the first to combine quantitative palynofacies and characterization of sedimentary organic matter. Their research was carried out in order to gain a better understanding of the depositional development throughout the upper part of the Botneheia Formation until the lower part of the Norian age Knorringfjellet Formation. Their study revealed seven palynofacies assemblages, including two for the upper Botneheia and the Tschermakfjellet formations.



## 2. Geological setting

### 2.1 Svalbard and the Barents Sea area

Svalbard represents an uplifted and exposed part of the northwestern corner of the Barents Sea Shelf (Faleide et al., 2008). The archipelago's crucial location and the poor coverage of vegetation, permits detailed geological studies. This contribute greatly to the understanding of the development of the Barents Shelf, as equivalents of the Triassic Svalbard successions are present throughout the Barents Shelf (Mørk and Worsley, 2006; Worsley, 2008). The sea level of the Barents Sea is relatively shallow, with an average depth of 230 meter (Sakshaug et al., 1994). The Barents Sea is bounded by the Svalbard archipelago in the northwest and Franz Joseph Land in the northeast. In the east, the sea borders to Novaya Zemlya (Faleide et al., 2008, Fig. 4). The Barents Shelf is divided into two main provinces: a western and an eastern region (Worsley, 2008). Faleide et al. (1984) divided the western Barents Sea into three regional geological provinces. These include an east- west trending basinal region, stretching from the Norwegian coast until 74°N. The second comprising a platform area north of 74°N, whereas the western continental margin makes out the third province (Faleide et al., 1984).

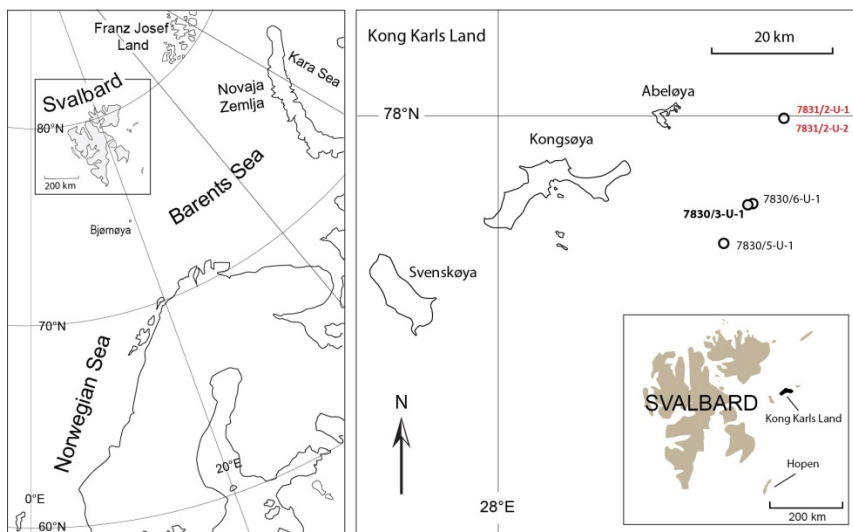


**Figure 4:** Location map the studied cores 7831/2-U-2 and 7831/2-U-1 offshore Kong Karls Land (figure courtesy of Dr. N. W. Paterson).

## 2.2 The Barents Sea area during the Triassic

Five major depositional phases took place throughout the late Paleozoic to present day in the western Barents Shelf region, forming the area and its successions as they appear today (Worsley, 2008). Since this study concerns the palynostratigraphy of the Middle to Late Triassic, the reader is referred to Worsley (2008) for information on the earlier and later geological development of the region, and for a more detailed description.

During the Triassic, the Barents Shelf area made up a vast epicontinental seaway (Glørstad-Clark et al., 2010). This seaway was located at the northwestern corner of the Pangaea supercontinent (Riis et al., 2008, Fig. 6a). Throughout the Triassic, the Pangaeian plate migrated towards north (Nystuen et al., 2008) while the seaway remained open in the north towards the Panthalassa Ocean, a precursor of the Pacific Ocean (Bagatikov et al., 2000). The seaway was bounded by Pangaea in the west, east and south (Riis et al., 2008, Fig. 6a).

From the Olenekian, all into the Carnian, major sediment supplies from east-southeast derived from the Uralian Orogeny and the Novaya Zemlya transformed this previously deep shelf area, into an extensive prograding paralic platform (Riis et al., 2008). Until the latest Ladinian, the Botneheia Formation was deposited in the still deep, western and northwestern parts of the shelf, where the large, prograding delta had yet to reach (Riis et al., 2008, Fig. 6b). In the mid-Carnian, the delta finally reached into Svalbard (Riis et al., 2008, Fig. 6c). Due to this progradation, the formations are older in the southeast than in the northwest, manifested as a diachronous boundary between the Middle and Upper Triassic Series (Riis et al., 2008).

Seismic data suggest that the deposition of the Botneheia Formation was of regional extent (Høy and Lundschieen, 2011) and that the formational top coincides with a regional seismic reflector (Lundschieen et al., 2014, Fig. 5). The high degree of cementation within the Botneheia Formation core 7831/2-U-2 may thus represent a widespread characteristic feature for the Botneheia Formation (Riis et al., 2008). Lundschieen et al. (2014) interpreted core 7831/2-U-2 to be from strata just below or close to the reflector (Fig. 5). Seismic data from the region show a system of major clinofolds, extending all the way from the Sentralbanken High area, almost until Kvitøya (northeast of Kong Karls Land) (Høy and Lundschieen, 2011).

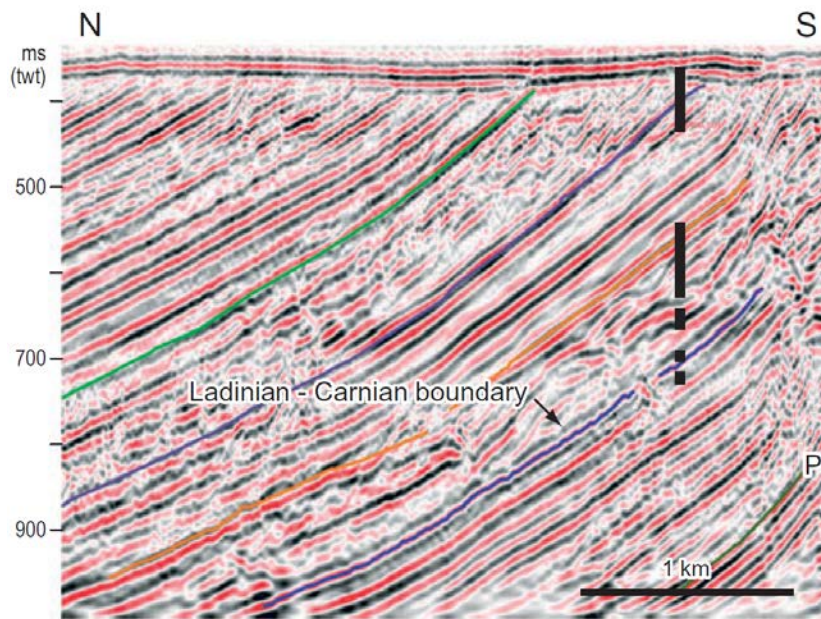


**Figure 5:** Seismic section from offshore Kong Karls Land, showing approximate position of the five cores drilled in the area. The two lowermost represent the cores in the present study. The purple reflector indicates the Ladinian – Carnian boundary (from Riis et al., 2008).

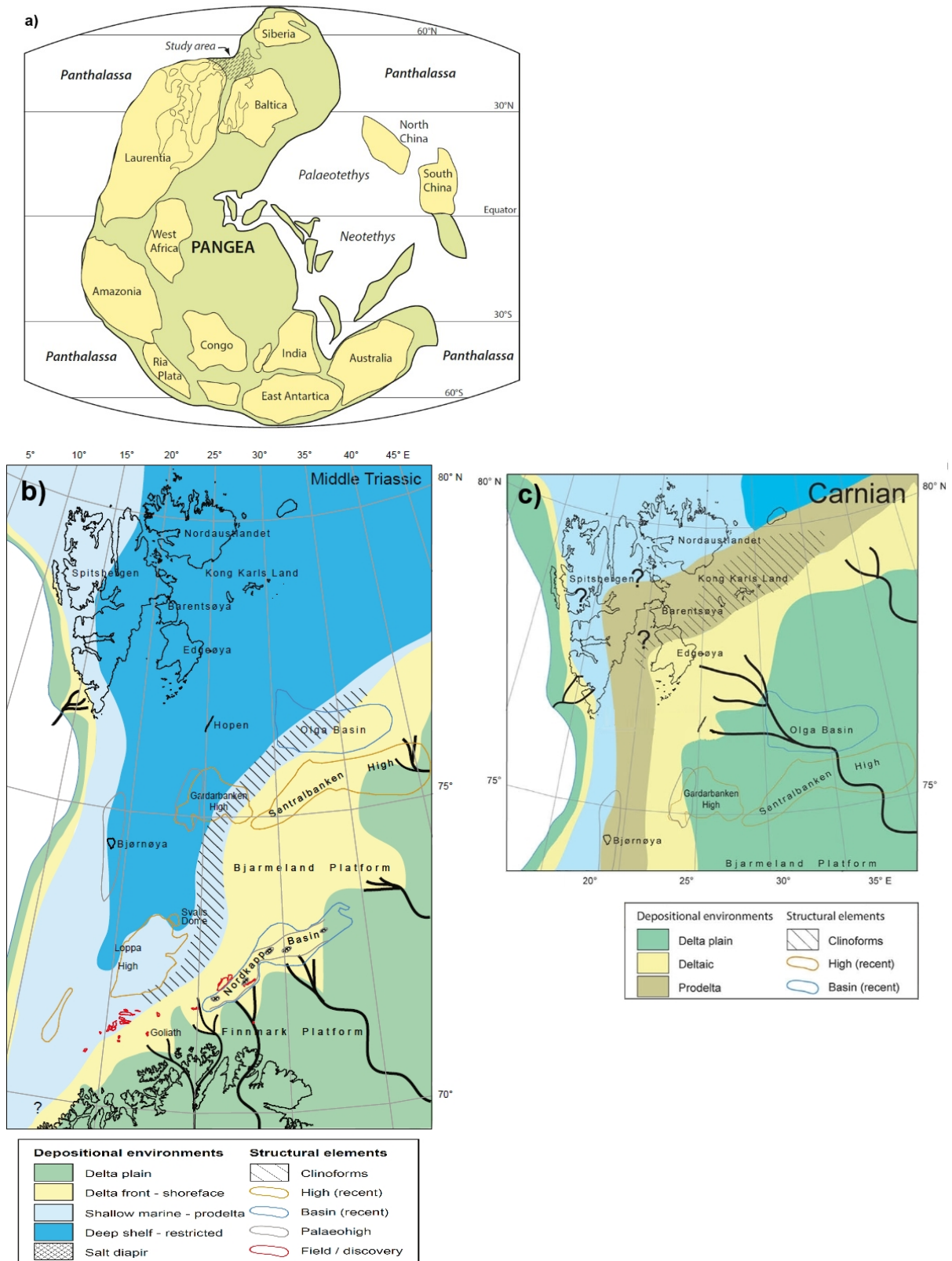


**Figure 6:** a) The Pangaea supercontinent during the Late Paleozoic, showing the evolution of the study area as a large embayment (Lundschieen et al., 2014). b) Reconstruction of the Middle Triassic palaeogeographic evolution of the Svalbard archipelago and the Barents Sea Shelf (from Lundschieen et al., 2014), c) Reconstruction of the Carnian palaeogeographic evolution of the Svalbard archipelago and the Barents Sea Shelf (modified from Klausen and Mørk, 2014).

## 2.3 The Triassic lithostratigraphy of Svalbard and the Barents Sea area

The Sassendalen and the Kapp Toscana groups comprises the Triassic successions present in Svalbard (Mørk et al., 1999). The Sassendalen Group has a total thickness of up to 700 meter in Svalbard and up to 1000 meter on the Barents Shelf. The group consists of shales, siltstones and sandstones of Early to Middle Triassic age. In western Spitsbergen, the group includes coastal to deltaic sedimentary rocks, grading into organic rich shelf mudstones towards east in Svalbard, and southwards on the Barents Shelf (Mørk et al., 1999). In eastern Svalbard and central Spitsbergen, the Sassendalen Group is represented by the Botneheia Formation (Pčelina, 1983). The Botneheia Formation comprises mainly black shales, making up a coarsening- upwards succession, with mudstones grading into siltstones. Thin, yellow weathering carbonaceous siltstone layers (Fig. 14b) and abundant phosphate nodules with a diameter up to three cm (Fig. 14c) occur throughout (Mørk et al., 1999). The Botneheia Formation comprises the Muen Member and the overlaying Blanknuten Member (Fig. 7). The Blanknuten Member has been dated to the Ladinian by ammonites and bivalves (Mørk et al., 1999). The member has a stratigraphic thickness of 21 meter in the stratotype section at Edgeøya and consists mainly of shale, calcareous siltstone and silty- limestone (Mørk et al., 1999). This highly calcareous character makes the member highly resistant to erosion. Thus, the member forms steep, pronounced cliffs where exposed in Svalbard (Mørk et al., 1999, Fig. 16c) and typically topographical highs when outcropping at the seafloor (Riis et al., 2008).

The overlying Kapp Toscana Group (Mørk et al., 1999, Fig. 7) has an approximate total thickness of up to 475 meter in Svalbard and up to 2000 meter on the Barents Sea Shelf (Mørk et al., 1999). The group comprises shales, siltstones and sandstones of Late Triassic to Middle Jurassic age (Mørk et al., 1999). The Storfjorden Subgroup comprises the compositionally immature lower part of the Kapp Toscana Group. This includes the Tschermakfjellet, De Geerdalen, Skuld and Snadd formations (Mørk et al., 1999, Fig. 7). The Tschermakfjellet Formation has been dated by ammonites to the early Carnian (Weitschat and Dagys, 1989; Dagys et al., 1993), and overlies the Botneheia Formation (Fig. 7) and the time-equivalent Bravaisberget Formation (Krajewski et al., 2007). The boundary between these two groups is

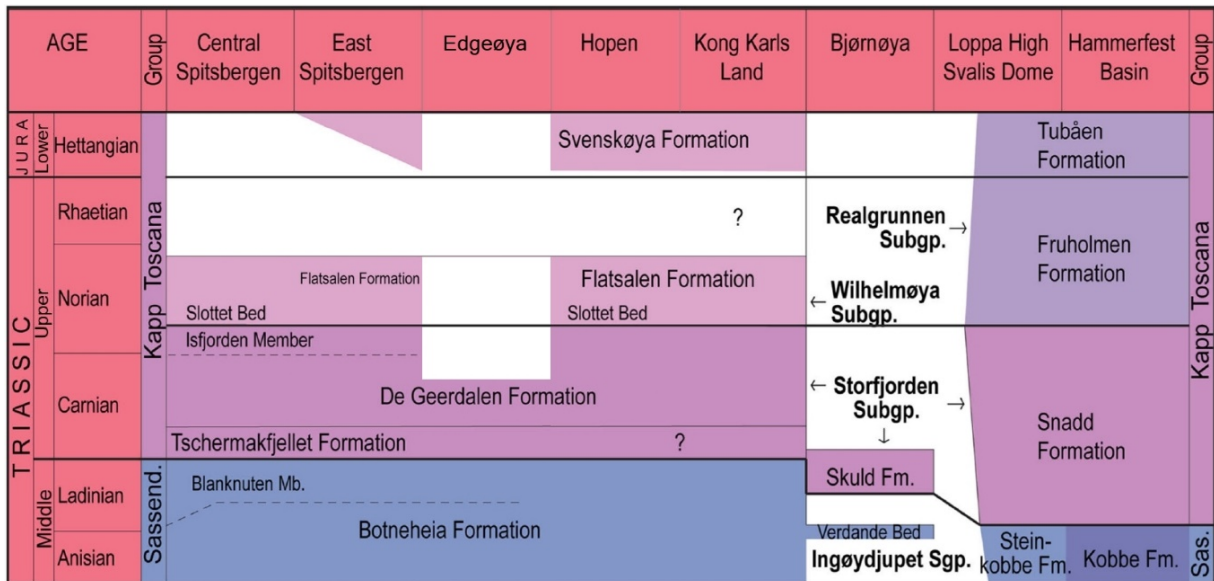


**Figure 7:** Lithostratigraphic scheme of the Middle Triassic to earliest Jurassic of Svalbard and the Barents Shelf (modified from Klausen and Mørk, 2014. Modifications based on Lundschieen et al., 2014).

time transgressive from the southern Barents Sea to Spitsbergen (Fig. 7) and coincides approximately with the Ladinian - Carnian transition in Svalbard (Riis et al., 2008). The Kapp Toscana Group constitutes late Middle Triassic to Middle Jurassic mudstones and sandstones of shallow marine to deltaic origin, indicating a major shift in the depositional regime throughout the entire Barents Shelf (Mørk et al., 1999).

### 3. Materials and methods

#### 3.1 Collection of material

During the last decade, the Norwegian Petroleum Directorate (NPD) has conducted regular expeditions to the Barents Sea area, including Svalbard. In 2005, the NPD drilled, with SINTEF Petroleum Research as operator, five shallow stratigraphic cores approximately 20 km east offshore Kong Karls Land (Riis et al., 2008, Figs.4 and 8), including the two cores of the present study. Their goal was to retrieve cores spanning the Permian-Triassic boundary. Instead, considerably younger cores were obtained. The cores were drilled in an area with a salt-cored structure, an ideal location for shallow stratigraphic drilling, as the salt movement brought the Middle and Upper Triassic successions up to the seafloor (Fig. 2). Palynological studies of shallow stratigraphic cores are of great importance as few Middle Triassic locations on Svalbard yield adequate samples suitable for dating and correlation (Vigran et al. 2014). The two studied cores were overlain by a few meters of Pleistocene tills (Riis et al., 2008), which has since been removed. The two cores were drilled approximately 200 meter apart, with an estimated stratigraphical gap of a few up to 30 meter between them (Xu et al., 2014, Fig. 23a) The core number 7831, indicates the latitudinal coordinate (78°N), and the longitudinal position (31°E) (Figs. 2, 4 and 8). Seventeen palynological samples were collected from the cores by SINTEF Petroleum Research in 2006, and 19 additional samples were later obtained in 2013 by the University of Bergen. Eighteen palynological slides were available from each of the two cores (Tables 2 and 3). The average sampling density of core 7831/2-U-2 is 0.70 meter, whereas that of core 7831/2-U-1 is of 0.86 meter. The studied stratigraphic cores are stored at the NPD core storage in Stavanger, Norway.

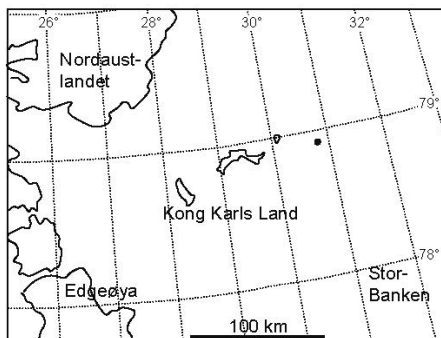


**Figure 8:** Location map of the shallow stratigraphic cores (black dot) offshore Kong Karls Land (modified from Riis et al., 2008).



## 3.2 Palynological preparation

The palynological slides from 2006 were processed at SINTEF Petroleum Research. The samples from 2013 were processed by Palynological Laboratory Services Limited, United Kingdom. No significant qualitatively or semi-quantitatively differences were observed between the two batches during this study.

Both sample sets were processed using standard palynological processing techniques (Doher, 1980). This method has proven to be the most efficient extraction technique of palynomorphs regarding absolute number of specimens and taxa (Riding and Kyffin-Hughes, 2011). The basics of the processing technique are to first separate the total organic residue from the minerals present. The next step includes separating the palynomorphs from the other organic matter (Traverse, 2007).

The initial processes of the technique starts with cleaning, disaggregation and weighing of the samples (Traverse, 2007, Fig. 9). The cleaning process includes at least one of three methods (Doher, 1980). These include washing the sample under running water, while brushing and then blowing the sample with compressed air. Another method is to scratch the sample using a knife and discard of all scrapings. The third method is to place crushed samples in distilled water for 10 minutes (Doher, 1980). The next step is the disaggregation process. This is performed to break the samples down to pea-sized fragments by using a clean mortar and pestle (Doher, 1980). The next main stage includes removal of the carbonates and the silicates (Fig. 9). The carbonate minerals are disaggregated by adding 10 % hydrochloric acid (HCl) to the sample in a beaker. When the carbonates have been successfully removed, the silicates can be disaggregated. This is done by adding hydrofluoric acid (HF) to the beaker (Doher, 1980). The residue is then treated ultrasonically, followed by oxidative maceration. The latter performed by nitric acid to further disintegrate and separate organic material from the palynomorphs (Doher, 1980). The final stage includes cleaning of the residues. Finally, the residues are mounted onto glass slides (Doher, 1980). The palynological processing technique is potentially hazardous, thus careful steps need to be undertaken (Doher, 1980). As the technique is described highly simplified herein, the reader is referred to Doher (1980) for a detailed systematic instruction on the subject.



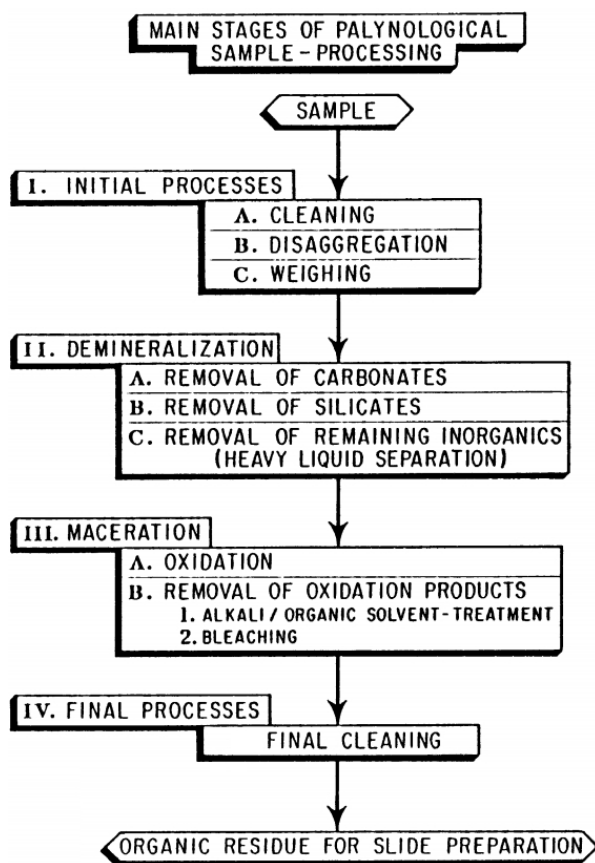


**Figure 9:** Basic steps of the standard palynological processing technique (modified from Traverse, 2007).

### 3.3 Microscopy and palynological analyses

The palynological and palynofacies analyses were carried out at the Department of Earth Science at the University of Bergen. A Zeiss Axioplan transmitted light microscope was applied.

The photographs were obtained with a Zeiss-Axio imager.A2 Axio Cam ERc 5s.

Transmitted light microscopy is still the most widely used method of analyzing palynomorphs, despite being one of the oldest techniques. The method provides an easily accessible and cheap way to examine palynomorphs, their structures and ornamentation (Coxon & Clayton, 1999). By shifting between different focuses, the ornamentations (exine patterns) of sporomorphs are highlighted. Focusing at high level makes protruding ornaments (sexine elements) appear bright (Lux), and the spaces (cavities in the tectum) between the protruding

elements relative dark (Obscuritas). When focusing at lower intensity, the opposite occurs (Fig. 10). This approach is called LO – analysis (L =lux/O = obscurus) (Hesse et al., 2009).

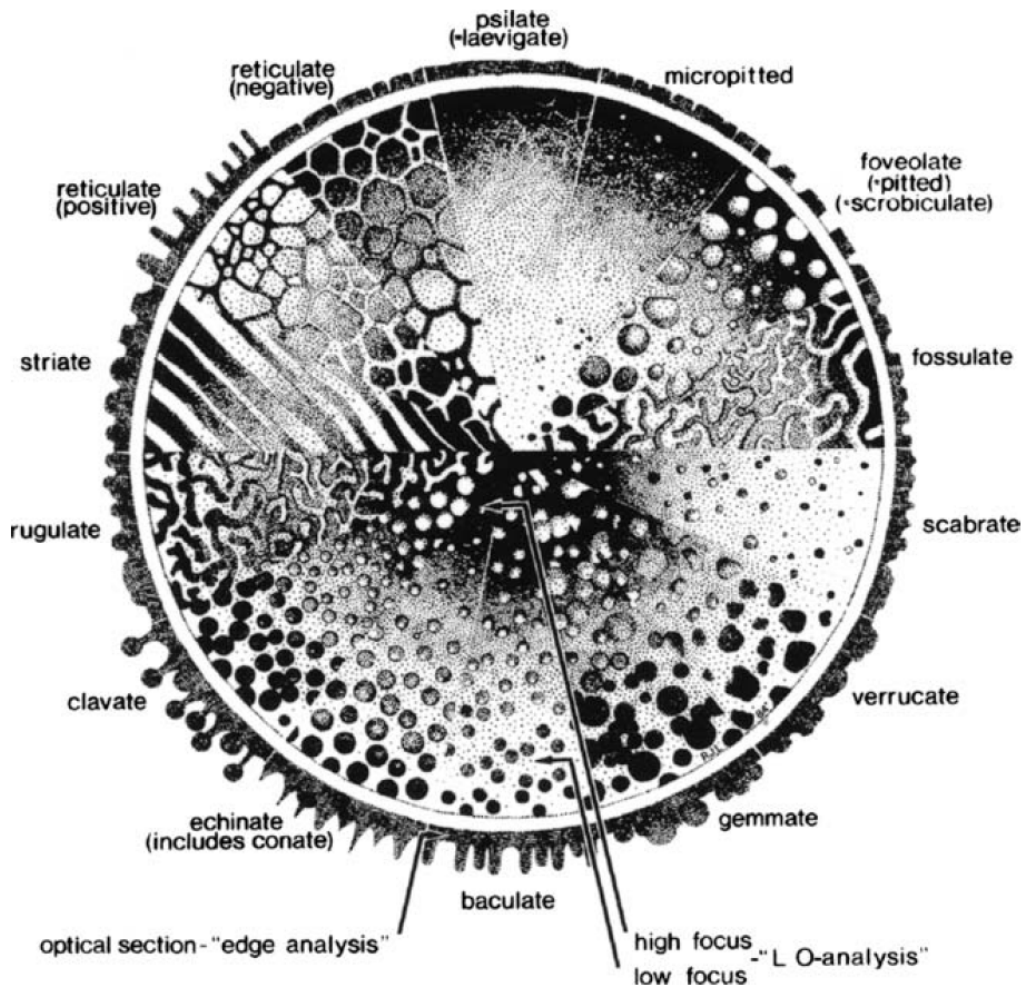


**Figure 10:** Different sculpture types as seen with varying levels of focus (from Traverse, 2007).

By focusing with moderate focus at the surface of the exine at the outer edge of the palynomorph, a verification of the conclusions from the LO- analysis can be obtained. This method is called “edge analysis” (Traverse, 2007, Fig. 10). Careful steps need to be carried out to ensure the reliability of palynological analysis. Precise identification of palynomorphs depends on correct methods of sampling, processing and analysis. Various factors contribute to unreliable samples. These may include reworking and mixing of assemblages in nature and contamination in the laboratory (Riding and Kyffin-Hughes, 2004). These factors must therefore be kept in mind during analysis.

By counting 200 palynomorph specimens for each palynological slide, semi-quantitative abundances were determined. Finally, the slides from core 7831/2-U-1 were analysed for rare taxa. Because almost all of the slides from core 7831/2-U-2 required a full scan to reach 200 specimens, the samples from this core were not rescanned.

Late Triassic palynofloras are highly diverse, and in combination with often poor preservation, identification of the various palynomorphs were challenging. Thus, the identification was often made on generic level, although identification to species level was highly attempted and possible for many of the samples. The palynomorphs recorded are plotted in a stratigraphic occurrence charts (Appendix III) created in the computer software StrataBugs, combined with the core logs, drawn in Adobe Illustrator CS6. The charts show the frequency distributions of the sporomorphs (Appendix III), and thus assist in the interpretation of depositional environment and palaeoclimatic conditions. This can be inferred based on the fact that certain plant groups are associated with certain parental plants of vegetational and climatic preferences (Tyson, 1995). The relative abundance variations of the counted palynomorphs are also shown in Pollen-Phytoplankton-Spore (PPS) ternary plots (Figs. 11 and 12). This is a widely used method to determine the relative distance between the source vegetation and the depositional environment (Batten, 1979; Tyson, 1993).

### 3.4 Palynofacies

The pioneering work of Muller (1959), led to the development of the palynofacies concept (Tyson, 1993). His work showed the importance of studying, not only the palynomorphs, but also the remaining particulate organic matter (POM) such as cuticles and tracheids in palynological preparations. By doing so, information can be acquired to supplement in the interpretation of facies and palaeoenvironment, and in palaeogeographic reconstruction (Tyson, 1993). Combaz (1964) introduced the palynofacies term, applying it to all organic material recognizable in palynological preparations (Ercegovac and Kostić, 2006). The concept has since then been redefined and elaborated by several authors. Tyson (1995) established

the modern concept of palynofacies (Batten and Stead, 2005). He defined it as a specific assemblage of palynological organic matter within sediment reflecting particular sets of environmental conditions (Tyson, 1995). In the last three decades, the application of palynofacies has increased considerably and is now widely used (Ercegovac and Kostić, 2006). Palynofacies analyses has the potential to detect and describe processes that took place simultaneously or at a later stage in relation to the formation of the organic facies. This will supplement in the evaluation of the source rock potential (Batten, 1980).

Throughout Earth's history, the conditions and factors involved in the composition, deposition and preservation of organic matter have changed significantly (Tissot and Welte, 1984). Hunt (1963) showed that the average weight percent of organic matter increase with decreasing particle size of the deposited sediments. The amount and quality is further dependent on the degree of primary production, biochemical degradation and depositional processes (Demaison and Moore, 1980). In addition, marine organic matter is more prone to biodegradation and degrades more rapid than derivatives of terrestrial sources (Ercegovac and Kostić, 2006). The study of all the processes that affect animal and plant remains as they become fossilized is called taphonomy (Martin, 1999). Because of the complexity of sedimentary organic matter, a precise determination of the concept is difficult to achieve.

For this study, a modified and simplified scheme of Tyson (1995) was applied (Table 1). Palynofacies analysis involves applying palynological techniques to study the depositional environment by evaluating the total assemblage of particulate organic matter present (Tyson, 1995). The palynofacies analyses were conducted by visually estimating the ratio between palynomorphs, phytoclasts and amorphous organic matter in the kerogen (un-oxidized) preparations. This was done in ten fields of view for each of the slides, and the average proportions were calculated. This is a common method for performing palynofacies analyses, and has certain advantages compared to traditional palynological counting. Firstly, it provides a quicker method, giving quick and reliable information about the palaeoenvironment. In addition, good preservation of the palynomorphs is not required, as long as they can be identified as such.

Tyson (1995) described the different dispersed palynological organic matter and provided a schematic key that was useful during the present study. The key applies mainly to thermally immature to slightly mature sediments, focusing especially on phytoclasts. Phytoclasts are particles of structured organic matter derived from plants (Tyson, 1993). The phytoclasts are divided into an opaque and a translucent category. The opaque phytoclasts are non-fluorescent, and may have signs of biostructures (e.g. pits). Oxidized or carbonized woody tissues (including charcoal) make up this subdivision. The translucent phytoclasts possess both definitive biostructure (such as wood tracheids and cuticles) and no definitive biostructure. Cuticles are the outermost “waxy” layer of leaves and stems of higher plants (Batten, 1996). They occur as sheets and are often pale yellow in colour. Wood tracheids (Fig. 21a) are generally lath to equant in shape, brown in colour and have pits (cavities) as internal structures. Phytoclasts with no definitive biostructure comprise of such as fibrous bundles (possibly seagrass), “membranes” (possibly cuticle or zooclast fragment), “pseudo-amorphous” phytoclasts (residual signs of structure) and what probably is wood tracheid tissue without visible pits (Tyson, 1995). Typical AOM in fine-grained, marine sediments is derived from phytoplankton and bacteria (Tyson, 1995). Higher plant secretions and decomposition products are also included in the amorphous group, but traditionally not referred to as “AOM” (Mendonça Filho et al., 2012). AOM is the most important hydrocarbon source in source rocks (Mendonça Filho et al., 2012).

The palynofacies results are displayed as AOM-Phytoclast-Palynomorph (APP) ternary plots (Figs. 21 and 23). Tyson (1989) applied APP plots to divide kerogen assemblages into eleven marine shale facies. Such plots give information about the source proximity of terrestrial organic matter and about the reducing and oxidizing state of the depositional subenvironments controlling preservation of AOM (Tyson, 1993).

**Table 1:** Classification of the palynofacies constituents (modified from Tyson, 1995)

Category		Source	Constituent		
Structured	Zooclasts	Zooplankton Zoobenthos	Graptolite debris Arthropod debris		
	Palynomorphs	Zoomorphs	Scolecodonts Tectin foraminiferal linings Chitinozoa		
			Organic-walled phytoplankton (including meroplankton)	Prasinophyte phycomata Chroococcale cyanobacteria Botryococcales Hydrodictyales	
		Dinocysts Acritarchs Rhodophyte spores			
		Sporomorphs		Miospores: microspores pollen Megaspores	
		Phytoclasts	Macrophyte plant debris	Cuticle/epidermal tissue Cortex tissues Secondary xylem (wood) Charcoal Biochemically oxidized wood	
	Fungal debris			Hyphae	
	Amorphous			Higher plant secretions	Resins
				Higher plant decomposition products	Humic cell-filling precipitates Humic extracellular precipitates
		("AOM")	Flocs		Organic aggregates
Phytoplankton	Facal pellets				
Bacteria	Cyanobacteria/Thiobacteria				

## 4. Results

### 4.1 Quantitative palynology

In general, the cores 7831/2-U-2 and 7831/2-U-1 yielded long-ranging taxa, occurring consistent throughout. Some minor quantitative variations occur, but these are thought to only reflect smaller regional variations in the palaeoenvironment and are thus not of zonal significance. The relatively short lengths of core 7831/2-U-2 and core 7831/2-U-1 lead to somewhat unreliable first appearance datums (FADs) and last appearance datums (LADs) in the semi-quantitative palynological analysis. This is especially true for LADs near the top and FADs near the base of the cores.

#### 4.1.1 Core 7831/2-U-2 (Botneheia Formation)

The palynological samples from core 7831/2-U-2 had in general poor preservation and poor to moderate recovery (Table 2). Nevertheless, counts for all depths were carried out (Appendix III). An additional set of palynological slides were available for all except two depths from this core (8.65 and 9.30 meter). Counts of both sets were often necessary in order to reach 200 specimens, because of poor recovery. In sample 5 from 14.89 meter (Table 2), only 150 specimens were present, but the count is still included in the range chart. The three constituents in this sample were multiplied by 1.33 to reach a total of 200, making it fit in the PPS ternary plot (Fig. 11). Poor preservation made identification to species level often difficult. Thus, identification was often made on generic level or subdivision-level as “bisaccate” spp.

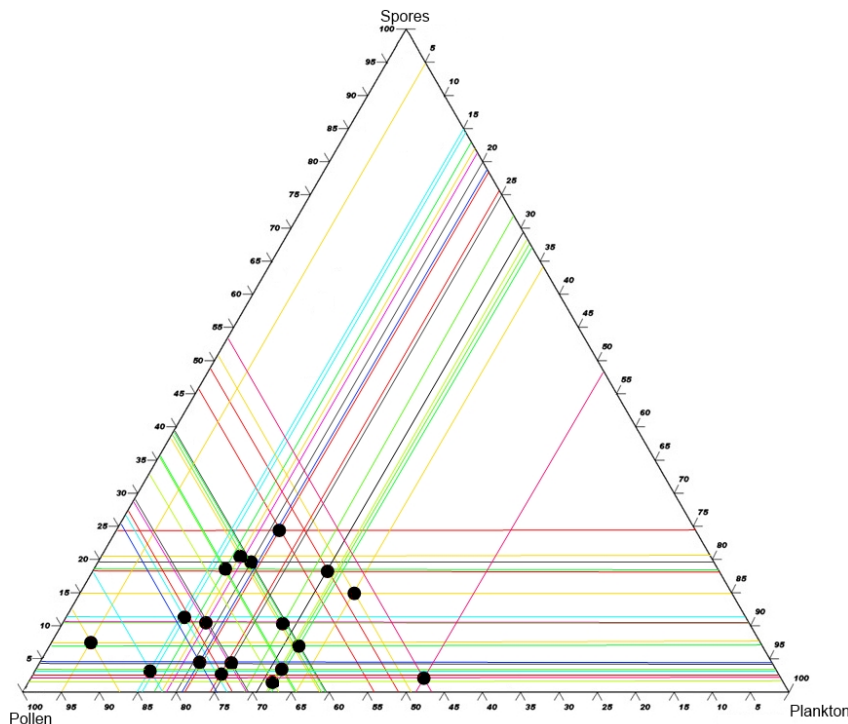


**Figure 11:** PPS ternary plots for core 7831/2-U-2, showing a general pollen dominance for the core.

The palynological assemblage recorded from this core was dominated by both alete and striate bisaccate pollen including *Alisporites* spp., *Staurosaccites quadrifidus*, *Striatoabieites balmei*, *Triadispora* spp., *Triadispora verrucata*. An upwards increase of the pollen *Ovalipollis* spp. was observed. The genus had its first occurrence at 16.75 meter and increased to abundant in the upper part (from 9.30 meter, Appendix II). Less abundant pollen species occurring relatively consistent throughout the assemblage included such as *Angustisulcites klausii*, *Araucariacites australis*, *Schizaeosporites worsleyi*, *Striatoabieites aytugi*, *Striatoabieites multistriatus*, *Chasmatosporites hians*, *Illinites chitinoides*, *Lunatisporites noviaulensis* and *Triadispora crassa*. A few specimens of *Echinitosporites iliacooides* occurred sporadically between 17.87 and 12.64 meter. The amount and diversity of spores increased greatly upwards. The most frequent occurring species was the trilete, smooth spore *Deltoidospora* spp. Marine prasinophytes, including the green algae *Crassosphaera* spp. and *Leiosphaeridium* spp., dominated together with the acritarch *Micrhystridium* spp. The algae *Tasmanites* spp. and the fresh water algae *Botryococcus* spp. occurred throughout the assemblage, but sporadically and rare.



**Table 2:** Sampling info and description of the palynological slides of core 7831/2-U-2

Formation	Sample depth (m)	Sampled by:	Sample date	Sample No.	General palynological description
Botneheia	6.16	SINTEF Petroleum Research	13.09.2006	18	Poor to moderate preservation & moderate recovery; AOM dominated + pollen & acritarchs
	6.21	SINTEF Petroleum Research	27.06.2006	17	Poor preservation & recovery; AOM dominated + pollen.
	6.83	SINTEF Petroleum Research	13.09.2006	16	Poor to moderate preservation & moderate to good recovery; AOM dominated + pollen.
	7.70	SINTEF Petroleum Research	27.06.2006	15	Poor preservation & good recovery; AOM dominated + <i>Crassosphaera</i> , spores & pollen.
	8.65	Uni. of Bergen (N.W.P)	09.09.2013	14	Poor preservation & good recovery; AOM dominated + <i>Crassosphaera</i> , acritarchs, spores & pollen.
	9.30	Uni. of Bergen (N.W.P)	09.09.2013	13	Poor preservation & moderate to good recovery; AOM dominated + <i>Crassosphaera</i> , spores & pollen.
	9.85	SINTEF Petroleum Research	27.06.2006	12	Poor preservation & moderate recovery; AOM dominated + <i>Crassosphaera</i> , spores & pollen.
	10.28	SINTEF Petroleum Research	13.09.2006	11	Poor to moderate preservation & recovery; AOM dominated + acritarchs, spores & pollen.
	11.43	SINTEF Petroleum Research	27.06.2006	10	Poor preservation & poor to moderate recovery; AOM dominated + acritarchs, spores & pollen.
	12.64	Uni. of Bergen (N.W.P)	09.09.2013	9	Poor preservation & good recovery; AOM dominated.
	13.45	Uni. of Bergen (N.W.P)	09.09.2013	8	Poor to moderate preservation & moderate recovery; AOM + pollen & <i>Crassosphaera</i> .
	13.88	SINTEF Petroleum Research	13.09.2006	7	Poor preservation & poor to moderate recovery; AOM dominated.
	14.32	SINTEF	27.06.2006	6	Poor preservation & poor to moderate recovery; AOM dominated.
	14.89	SINTEF	27.06.2006	5	Poor preservation & poor recovery; AOM dominated.
	15.65	Uni. of Bergen (N.W.P)	09.09.2013	4	Poor to moderate preservation & moderate recovery; AOM dominated.
	16.75	Uni. of Bergen (N.W.P)	09.09.2013	3	Poor preservation & moderate recovery; AOM dominated.
	17.87	SINTEF	13.09.2006	2	Poor preservation & recovery; AOM dominated.
18.79	SINTEF	27.06.2006	1	Poor preservation & recovery; AOM dominated.	

#### 4.1.2 Core 7831/2-U-1 (Tschermafjellet Formation)

The palynological samples from core 7831/2-U-1 showed in general moderately good recovery and preservation (Table 3). The palynological assemblages recorded showed an upwards increase in terrestrial palynomorphs of pteridophyte spores, coupled with a relative decrease in the abundance of marine palynomorphs. The palynological assemblage from the lower interval of the core (from the base until 14.78 meter; samples 1-10, Table 3) generally showed a regular upwards increase in the abundance of spores, coupled with a regular decrease of marine palynomorphs (Fig. 12). Acmes of the acritarch *Micrhystridium* spp. occurred regularly in the lower interval. The prasinophyte *Leiosphaeridia* spp. occurred abundantly consistent throughout the interval, together with common *Crassosphaera* spp. At 22.83 meter, a single specimen of the pollen *Echinosporites iliacooides* was recorded. A marked shift in the association was observed upwards from approximately 14.78 meter (samples 11-18, Table 3). Pteridophyte spores and gymnosperm pollen dominated this upper part of the core. The pollen species included such as *Alisporites* spp., *Aulisporites astigosus*, *Granasporites magnus*, *Illinites chitinooides*, *Podosporites amicus*, *Striatoabieites balmei*, various species of the *Triadispora* group and the monosulcoid pollen *Chasmatosporites* spp.

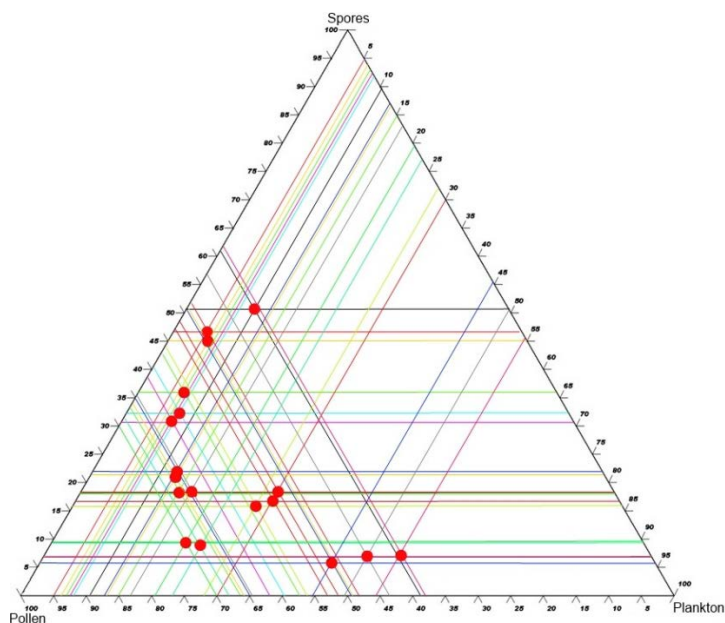


**Figure 12:** PPS ternary plots for core 7831/2-U-1, showing a dominance of pollen and marine palynomorphs, with a gradual increase of spores.

The spores included taxa and genera such as *Calamospora tener*, *Conbaculatisporites* spp., *Deltoidospora* spp., *Dictyophyllidites mortoni*, *Leschikisporis aduncus*, *Punctatisporites* spp., *Striatella seebergensis* and various species of the *Krauselisporites* group. Pollen such as the bisaccate striate *Lunatisporites noviaulensis* and *Schizaeoisporites worsleyi*, and the spore *Baculatisporites* spp. occurred consistent but rarely throughout. Sporadic and rare pollen such as *Tetrasaccus* spp. and *Cycadopites* spp. also occurred. Various spores including *Kyrtomisporites laevigatus*, *Aratrisporites* spp., *Aratrisporites laevigatus* and *Camarozonosporites laevigatus* occurred rarely but sporadic throughout the assemblage. The prasinophyte *Leiosphaeridia* spp. occurred throughout, whereas the prasinophyte *Crassosphaera* spp. and the acritarch *Micrhystridium* spp. occurred rarely, only in the upper part of the assemblage (from 10.82 meter). Other sporadic and rare occurrences of marine palynomorphs include the acritarchs *Cymatiosphaera* spp., the algae *Pterospermella* spp. and fresh water algae *Botryococcus* spp.

Appendix I contains a complete taxonomical list of palynomorphs present in the two cores.

**Table 3:** Sampling info and description of the palynological slides of core 7831/2-U-1

Formation	Sample depth (m)	Sampled by:	Sample date	Sample No.	General palynological description
Tschermafjellet	8.05	Uni. of Bergen (N.W.P)	09.09.2013	18	Moderately good preservation & recovery; spores & pollen.
	8.70	Uni. of Bergen (N.W.P)	09.09.2013	17	Moderately good preservation & recovery; spores & pollen.
	10.82	Uni. of Bergen (N.W.P)	09.09.2013	16	Good preservation & recovery; spores & pollen.
	11.85	SINTEF Petroleum Research	13.09.2006	15	Excellent preservation & good recovery; spores & pollen.
	12.98	Uni. of Bergen (N.W.P)	09.09.2013	14	Moderately good preservation & good recovery; spores & pollen + oxidized woody tissues.
	14.14	Uni. of Bergen (N.W.P)	09.09.2013	13	Good preservation & moderate recovery; spores & pollen + AOM.
	14.45	Uni. of Bergen (N.W.P)	09.09.2013	12	Varying preservation & good recovery; spores & pollen + oxidized woody tissues.
	14.78	SINTEF Petroleum Research	13.09.2006	11	Varying preservation & good recovery; spores & pollen.
	16.25	Uni. of Bergen (N.W.P)	09.09.2013	10	Poor preservation & recovery; spores & pollen.
	17.48	Uni. of Bergen (N.W.P)	09.09.2013	9	Moderate to good preservation & recovery; AOM, acritarchs, spores & pollen.
	19.61	SINTEF Petroleum Research	13.09.2006	8	Good preservation & recovery; AOM dominated + <i>Crassosphaera</i> spp., spores & pollen
	19.73	Uni. of Bergen (N.W.P)	09.09.2013	7	Good preservation & recovery; AOM dominated + <i>Crassosphaera</i> spp., spores & pollen
	20.95	Uni. of Bergen (N.W.P)	09.09.2013	6	Moderately good preservation & good recovery; acritarch dominated.
	22.83	Uni. of Bergen (N.W.P)	09.09.2013	5	Moderately good preservation & recovery; AOM dominated + pollen & spores.
	24.15	Uni. of Bergen (N.W.P)	09.09.2013	4	Poor- moderately good preservation & good recovery; acritarchs, pollen + AOM.
	24.33	SINTEF Petroleum Research	13.09.2006	3	Moderately good preservation & good recovery; AOM
26.56	SINTEF Petroleum Research	13.09.2006	2	Moderately good preservation & good recovery; acritarchs, pollen + AOM.	
27.95	Uni. of Bergen (N.W.P)	09.09.2013	1	Moderately good preservation & good recovery; acritarchs + AOM.	

## 4.2 Core description

The cores 7831/2-U-2 and 7831/2-U-1 were studied and logged during a few days in October 2014. Other authors have previously presented logs of the cores (Riis et al., 2008; Lundschieen et al., 2011; Xu et al., 2014) and discussed the cores in regards of various topics (e.g. Vigran et al., 2008; Høy and Lundschieen, 2011). The Svalbard lithostratigraphic terminology is applied for both cores, following the convention of the previous workers. Despite the fact that the cores represent the subsurface of the Barents Sea, which applies a different lithostratigraphic subdivision (Fig. 7). The similarity to outcrops in eastern Svalbard is striking (Riis et al., 2008). As the cores have not yet been made public by the NPD, only selected pictures of important features are presented herein.

### 4.2.1 Core 7831/2-U-2

Core 7831/2-U-2 comprises 13.3 meter of the Botneheia Formation (Riis et al., 2008). It consists of dark gray, laminated calcareous shale, with good to excellent organic richness (Lundschieen et al., 2014). Ovoidal to lenticular phosphate nodules are abundant throughout (Figs. 14 and 15), together with chert horizons and nodules, pyrite and thin calcite veins.

The core shows great similarity to the Botneheia Formation as described from Edgeøya (Riis et al., 2008) (Fig. 15c) and shows close resemblance with the Blanknuten Member (oral communication; Lundschieen and Mørk, 2015). Krajewski (2008) distinguished between four common texture types of the phosphogenic facies in the Blanknuten Member, based on studies from Edgeøya. These include peloidal and massive nodules, or nodules dominated by radiolarian (Figs. 16c and d) and pelecypod-shell. In core 7831/2-U-2, massive phosphatic nodules are the most common, in addition to nodules possibly derived from siliceous sponges, which are not occurring on Edgeøya (Riis et al., 2008, Figs. 14a, 14c, 15a-b). The massive nodules constitute of scattered mineral grains and organic and skeletal components in a matrix of homogeneous phosphate (Krajewski, 2008). Some of the phosphate nodules show pyritization (Fig. 15c).

Between 14.35 and 15.55 meter, the algae *Tasmanites* spp. can be observed macroscopically as dark brown dots (Fig. 14c). They occur abundant in this interval, observed as rock-forming flattened grains (Figs. 14c and 16a). However, no peak is observed for *Tasmanites* spp. in the palynological analysis within this interval. This is most likely caused by their large size, being up to 500 micrometres in diameter (Fig. 16a), thus, most of the *Tasmanites* were probably sieved out during the palynological preparation process, only leaving smaller specimens behind. Fossils, mainly bivalves, are present throughout the core, but no bioturbation is observed. Similar characteristics have previously been observed within the Botneheia Formation elsewhere in Svalbard (Krajewski, 2008, Figs. 16b and 15c). Two ammonites have been obtained from the core at 12.30 and 9.40 meters (Xu et al., 2014, Figs. 14a-b). At the very top of the core, a six cm thick layer of yellow weathering carbonaceous siltstone occurs. A similar layer is also present between 16.30 and 16.25 meter (Fig. 15b). These kind of weathering siltstones are common in the Botneheia Formation and the Blanknuten Member (Mørk et al., 1999).

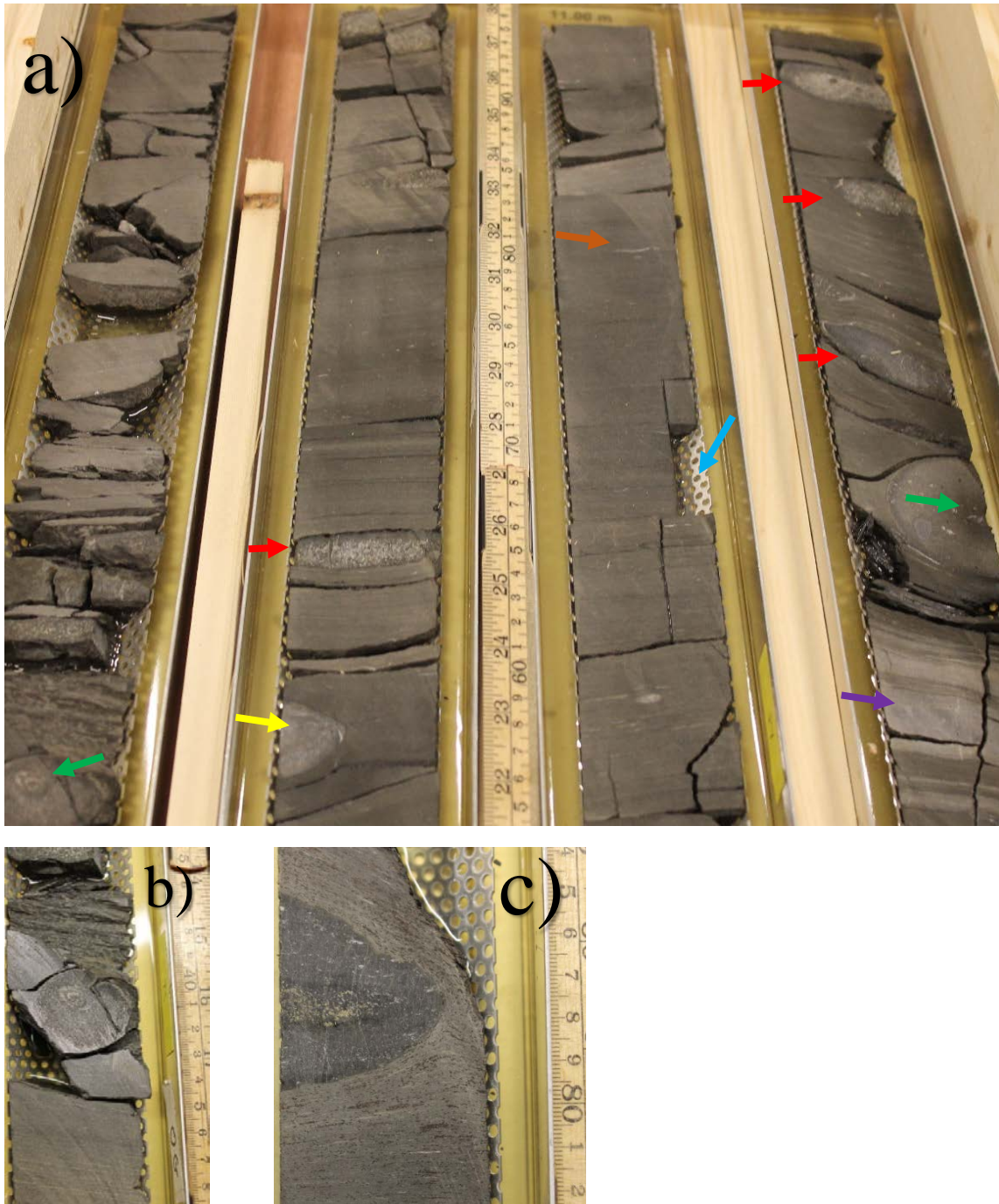


**Figure 13:** a) Core 7831/2-U-2, showing the upper parts of the intervals between 12 and 9 meter. Red arrows indicate nodules interpreted by Riis et al. (2008) to possibly be derived from siliceous sponges. The blue arrow shows an interval sampled for the Re-Os dating. Green arrows show ovoidal phosphate nodules from which ammonites have previously been obtained (Xu et al., 2014). The yellow arrow shows a massive phosphate nodule, the brown arrow a bivalve and the purple arrow shows siltstone. b) Ovoidal phosphate nodule in core 7831/2-U-2 at 9.40 meter depth. An ammonite has previously been obtained from this nodule. c) Phosphate nodule encompassed by abundant macroscopic algae *Tasmanites* spp. in the matrix, from 14.80 meter in core 7831/2-U-2.



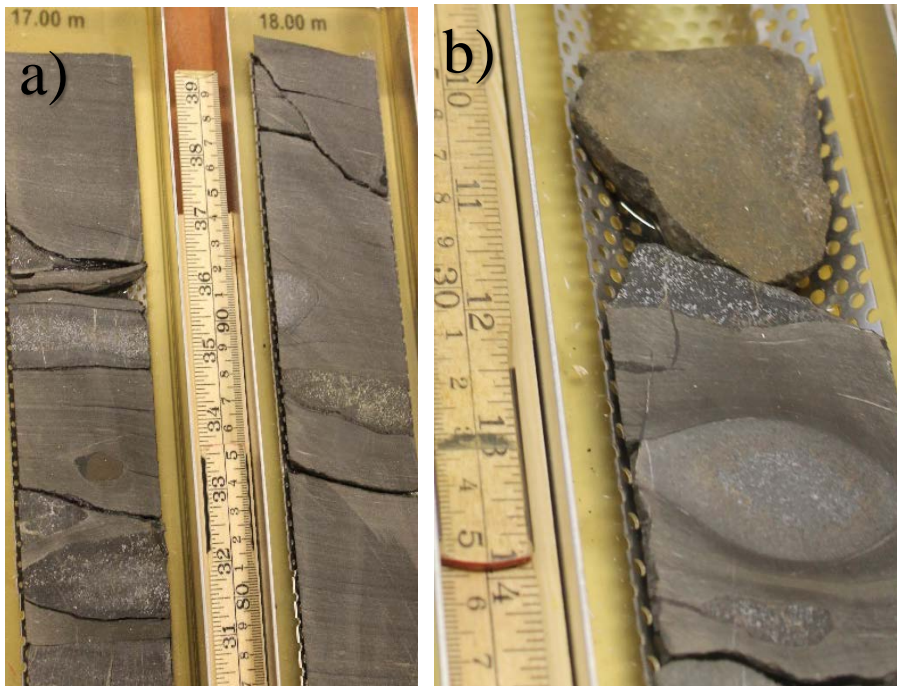


**Figure 14:** **a)** The intervals between 17.00 – 17.23 and 18.00 – 18.23 meter in core 7831/2-U-2, showing elongated nodules. **b)** The interval between 16.37 until 16.25 meter of core 7831/2-U-2, showing yellow weathering carbonaceous siltstone and phosphate nodules. **c)** Blanknuten, Edgeøya: The Blanknuten Member of the Botneheia Formation, containing abundant phosphate nodules and a major lensoidal carbonate (dolomitic) cementstone in dark gray mudstone and shale.



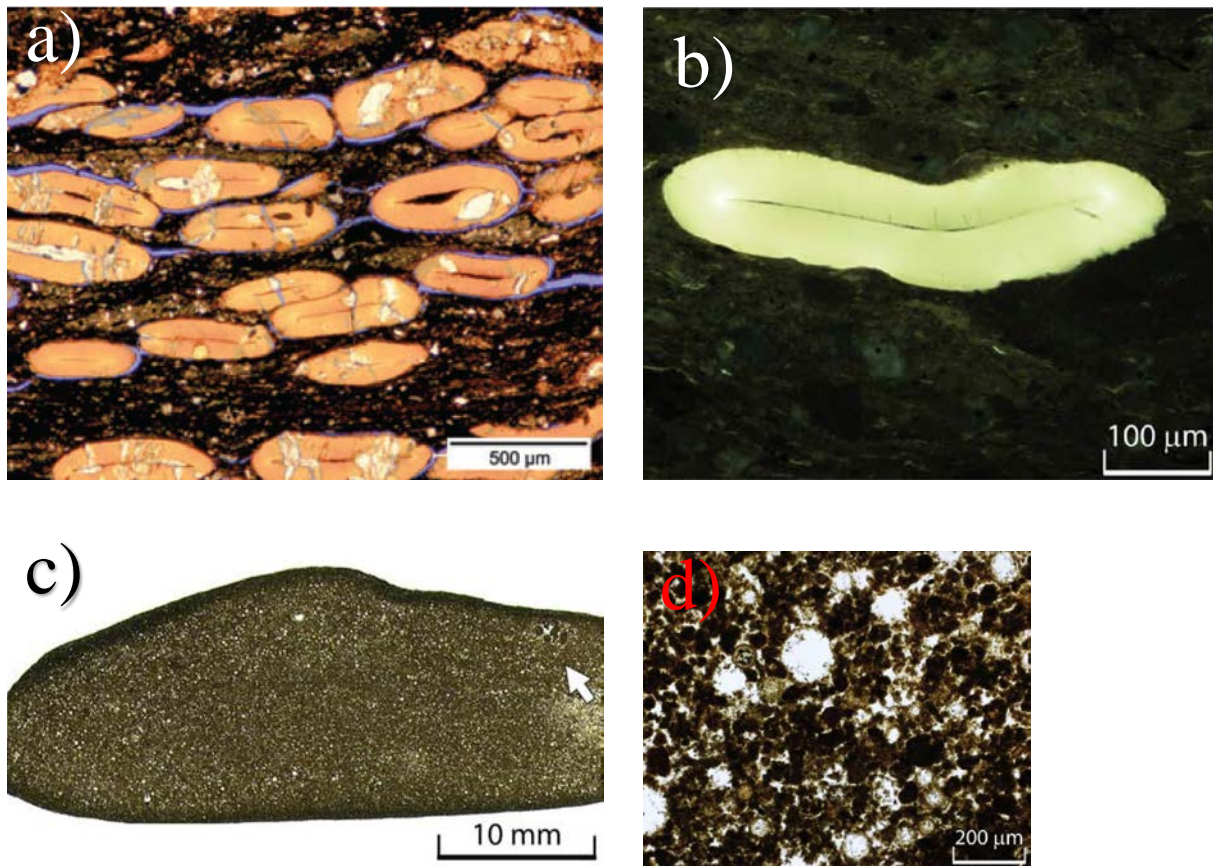


**Figure 15:** Transmitted light photomicrographs from the Botneheia Formation. **a)** Flattened *Tasmanites* in black claystone from core 7831/2-U-2 from approximately same depth as in Fig. 14b (photo from Vigran et al., 2008). **b)** Flattened *Tasmanites* from the Blanknuten Member on Edgeøya (photo from Krajewski, 2013). **c)** Thin section photo of a pristine phosphate nodule from the Blanknuten Member on Edgeøya. On Edgeøya, these occur abundantly as shown in Fig. 15c. In the central part of the nodule, the original texture of radiolarian-rich sediment is preserved, whereas in the outer parts mechanical orientation has taken place. The arrow indicate a cross section of a burrow filled with fecal pellets (photo from Krajewski, 2013). **d)** Matrix of the phosphate nodule in e) showing radiolaria (white dots) and abundant, phosphatized zooplanktonic fecal pellets. Late diagenetic calcite cement fills the remaining pore space (photo from Krajewski, 2013).

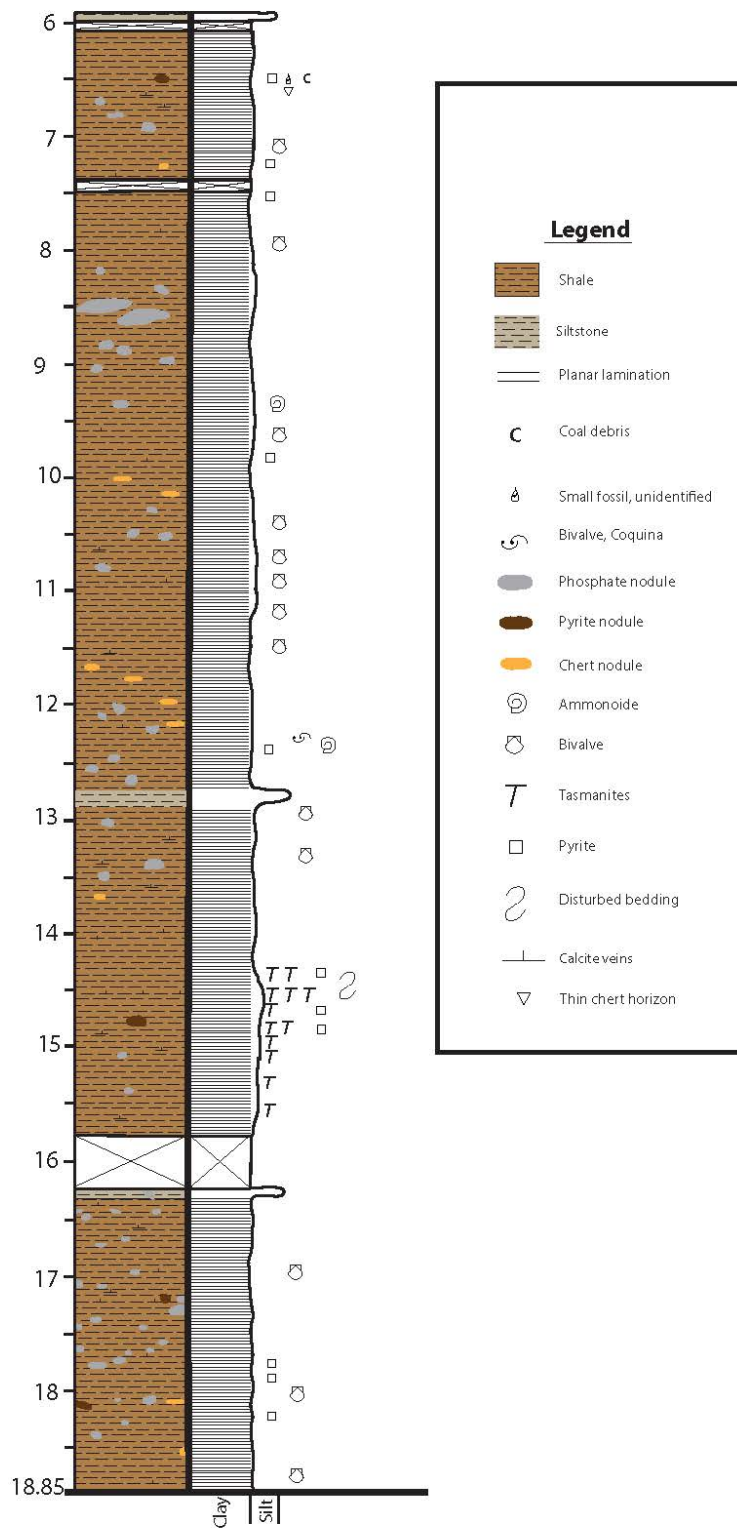
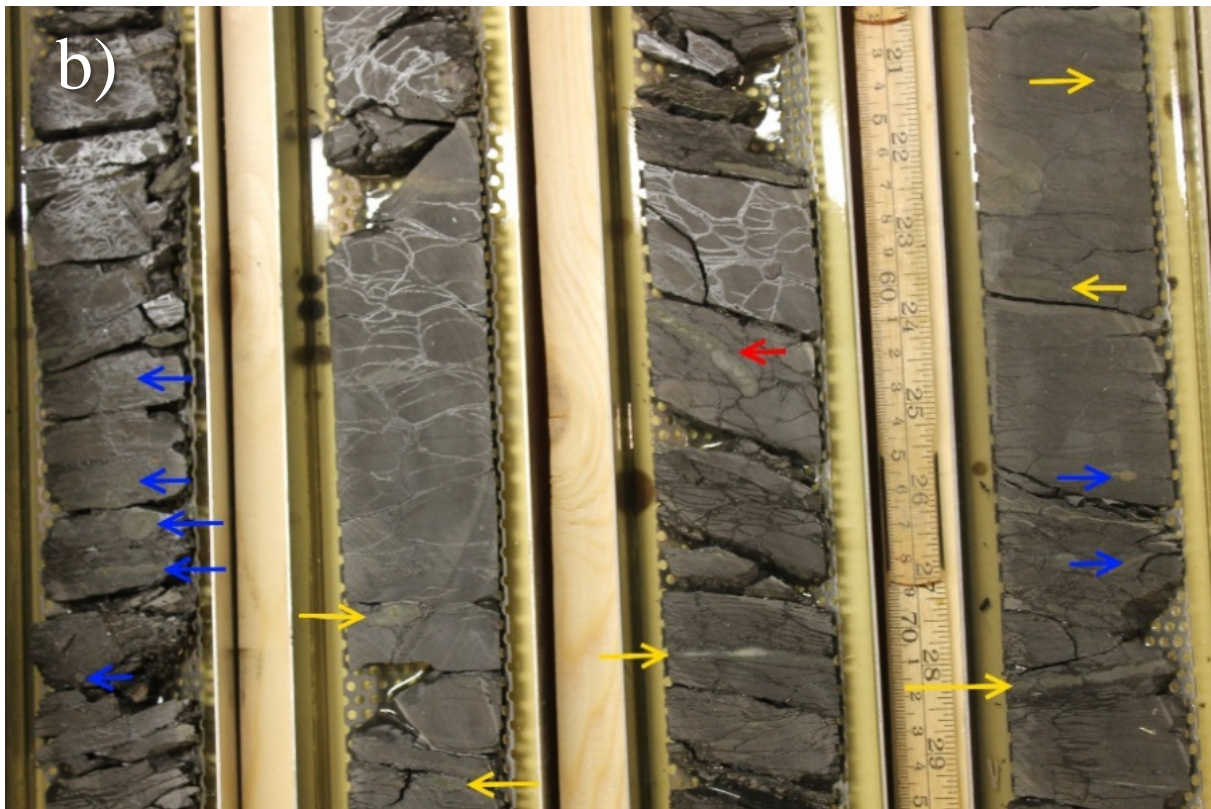
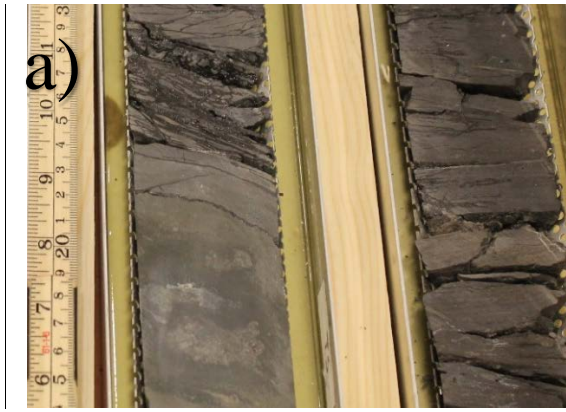


Figure 16: Log of core 7831/2-U-2, representing the Botneheia Formation.

### 4.2.2 Core 7831/2-U-1

Core 7831/2-U-1 comprises 19.95 meter of shale, silty sandstone and siltstone correlated to the Tschermakfjellet Formation (Riis et al., 2008, Fig. 24). The core is lithologically divided into three distinct intervals, a shale unit between 27.95 and 14 meter (Fig. 18) which is divided in two parts separated at 19 meter. The third and uppermost interval (upwards from 13.25 meter) comprises of immature silty sandstone and siltstone. The lower interval (from 27.95 to 19 meter) consist of gray, laminated shale, with low to moderate organic content, reflected by the lesser dark colour compared to the underlying core 7831/2-U-2. Pyrite and slickenside-surfaces occur throughout, together with sporadic, low degree of bioturbation. Phosphate nodules (Fig. 17b) and cherty horizons occur in this interval, but are more sparse compared to the underlying core 7831/2-U-2 and as reported from the Botneheia Formation on Edgeøya (Krajewski, 2008). The nodules decrease in abundance upwards within the interval. As such nodules are absent in the Tschermakfjellet Formation (Mørk et al., 1999), Xu et al. (2014) proposed that this lower interval could represent the gradual transition from the Botneheia Formation to the Tschermakfjellet Formation. The upper interval between 19 and 14 meter is lithologically different compared to the shale from the interval below as well as from the underlying core 7831/2-U-2, as phosphate and chert nodules are not recorded. This interval also has an even lower organic content compared to the interval below. Sparse fossil and siderite beds, combined with abundant pyrite, makes the shale resemble the Tschermakfjellet Formation as described by Lock et al. (1978). The third and uppermost interval between 13.25 and 8.00 meters, comprised an upwards grading into very fine grained sand- and siltstones. This interval often contains disturbed bedding and pyrite (Figs. 18 and 21). Some bioturbation and coal- debris are present sporadically (Fig. 21). The uppermost part is made up of strongly fractured sections (Fig. 21).



**Figure 17:** **a)** Sections of core intervals at 26.70– 26.86 and 27.70– 27.86 meter, showing a major, massive phosphate nodule and shale with calcite veins and minor pyrite. **b)** Sections of core intervals at 24- 27 meter of core 7831/2-U-1. The nodular structure (red arrow) resemble phosphatized *Thalassinoides* trace. Abundant chert horizons and nodules (yellow arrows) and pyrite (blue arrows)



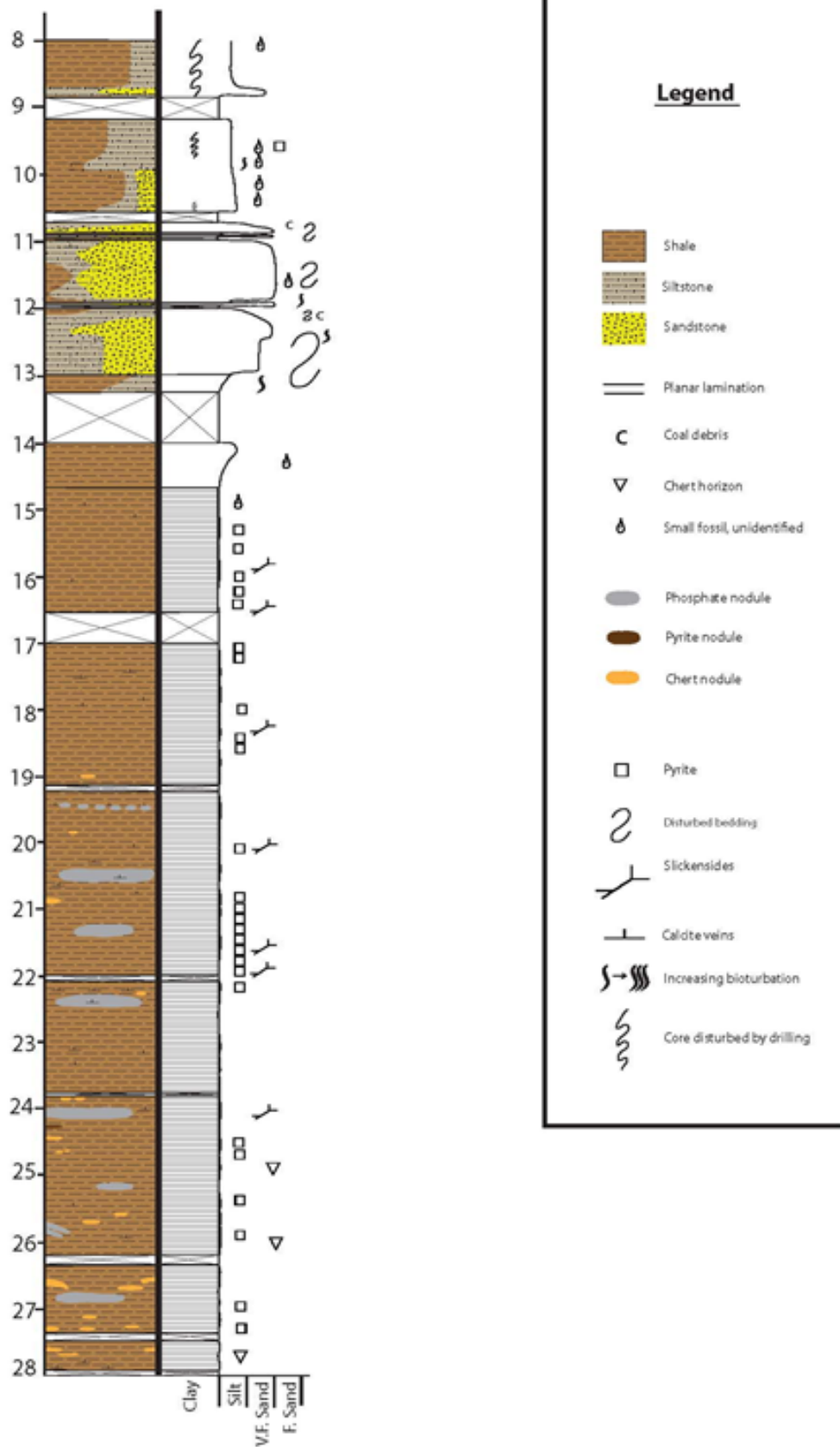


**Figure 18:** Log of core 7831/2-U-1, representing the Tschermakfjellet Formation.



**Figure 19: a)** The interval between 19.38 and 19.50 meter in core 7831/2-U-1, comprising mudstone with calcite veins and phosphate nodule horizon, possibly formed as tunnel infillings. **b)** The uppermost 30 cm of the interval between 15 and 12 meters in core 7831/2-U-1, showing sandstone, siltstone, pyritic mudstone and highly fractured shale.

### 4.3 Palynofacies analysis

The palynofacies groups observed included palynomorphs, phytoclasts and amorphous organic material. No zooclasts were observed. The observed phytoclasts (Table 4) comprised oxidized or carbonized woody tissues, wood tracheid tissue without visible pits, cuticles, pseudo-amorphous phytoclasts, “membranes”, fibrous bundles and wood tracheids with biostructures (pits). Since the ratios between the pollen and spores were documented in the counts, they were grouped as sporomorphs in the palynofacies analysis. All marine palynomorphs were recorded as phytoplankton. The amorphous organic matter observed, was almost exclusively of “typical AOM” nature (Table 1). Amorphous organic matter derived from higher plants (resins and humic precipitates) was much scarcer. This is especially true for core 7831/2-U-2. For convenience, all amorphous organic matter is referred to as AOM hereafter.

**Table 4:** Subdivision of the observed phytoclasts of the performed palynofacies analysis (based on Tyson, 1995)

<b>Phytoclasts</b>	Opaque		Oxidized or carbonized woody tissues
	Translucent	No definitive biostructure	"Pseudo-amorphous" phytoclasts
			Fibrous bundles
			Wood tracheid tissues without pits
			"Membranes"
		Definitive biostructure	Wood tracheids with pits
		Cuticles	

### 4.3.1 Core 7831/2-U-2

The palynofacies analyses results from core 7831/2-U-2, are presented in an APP diagram (Fig. 20). Six kerogen slides were available and analysed. All the samples plotted in field IX (distal suboxic-anoxic basin, Fig. 20) and were almost entirely dominated by AOM (Fig. 21b). In average, AOM comprised 99 percent of the total volume of organic particles in the samples. The recorded palynomorphs consisted mostly of sporomorphs, mainly bisaccate pollen, but phytoplankton was also present sporadically. The phytoclasts mostly comprised oxidized or carbonized woody tissues. However, rare wood tracheid tissue without visible pits, cuticles, “pseudo-amorphous” phytoclasts and “membranes” also occurred.

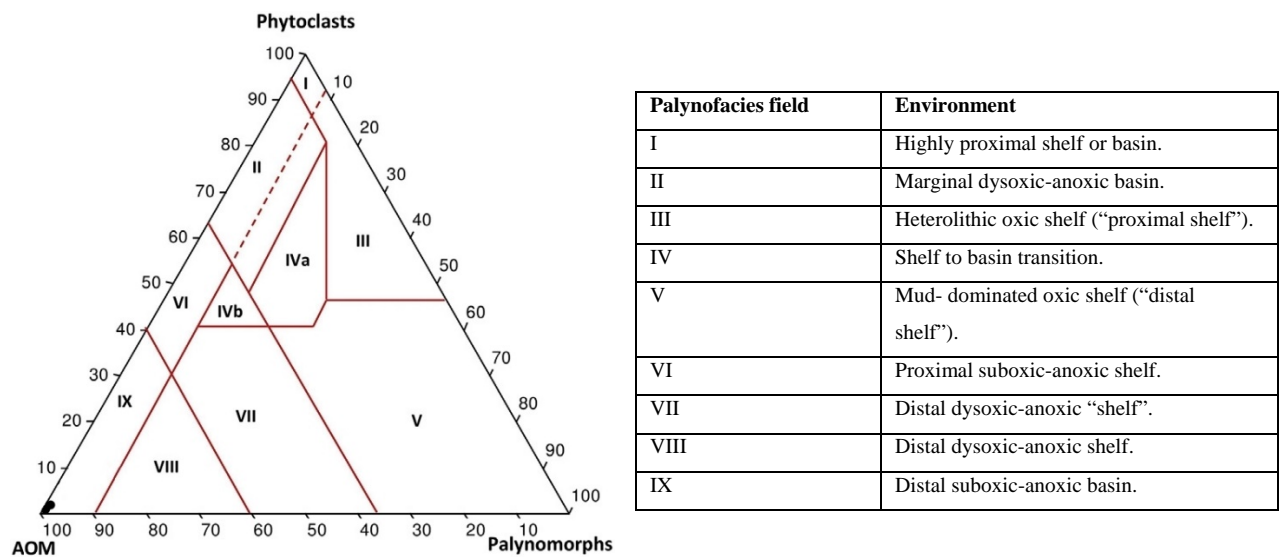


**Figure 20:** APP plots for the palynofacies analysis results for core 7831/2-U-2, showing a total dominance of AOM. The corresponding palaeoenvironments for the various fields are included (after Tyson, 1995).



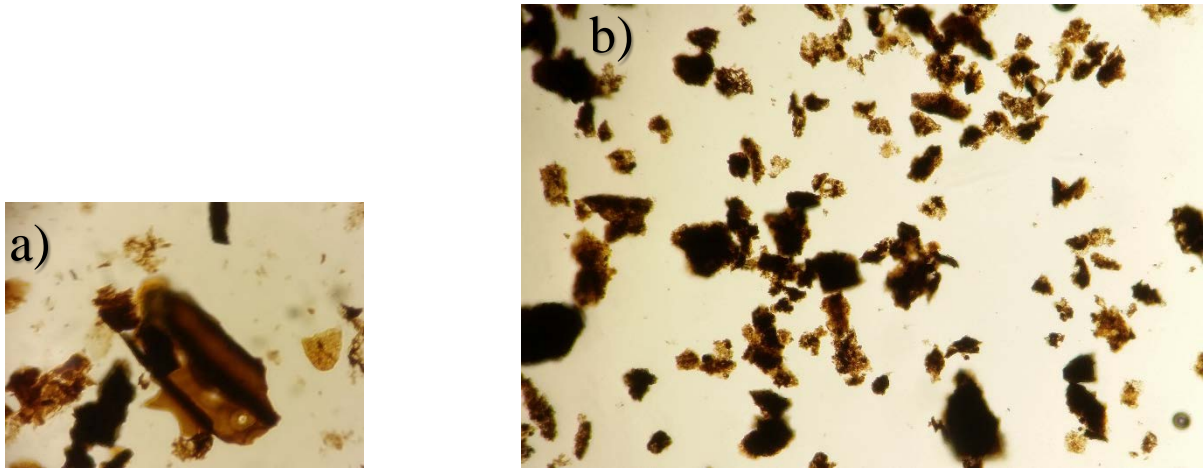


**Figure 21: a)** Palynofacies from 14.45 meter in core 7831/2-U-1, showing wood tracheid with pits, oxidized woody tissues, pollen fragment and AOM. **b)** Palynofacies from 12.64 meter in core 7831/2-U-2, showing domination of AOM.

#### 4.3.2 Core 7831/2-U-1

The palynofacies analysis of core 7831/2-U-1, assigned to the Tschermakfjellet Formation, are presented in an APP diagram (Fig. 22). Thirteen samples were analysed. The seven lowermost samples (27.95 to 16.25 meter) showed an almost entirely dominance of AOM, and contained only two percent phytoclasts and two percent palynomorphs in average. Thus, plotted in field IX (Fig. 22). In sample 14.45 meter, a significant increase in phytoclasts and palynomorphs occurred. At this level, phytoclasts amounted to 33 percent and palynomorphs eight percent of the total assemblage (Fig. 22). Thus, the sample plotted in field VI. In the sample above (14.14 meter) AOM dominated with 95 percent and plotted in field IX. The sample from 12.98 meter contained an increased proportion of phytoclasts and palynomorphs, with 32 and 5 percent, respectively. While the above sample (10.82 meter) showed a slight change with 30 and 9 percent, respectively. Hence, the two samples plotted in field IX (Fig. 22). In the second uppermost sample (8.70 meter), phytoclasts constituted 54 percent of the organic material. In this sample, AOM and palynomorphs amounted to 25 and 21 percent, respectively, plotting in field IVa (Fig. 22). In the uppermost sample (8.05 meter), the amount of palynomorphs and

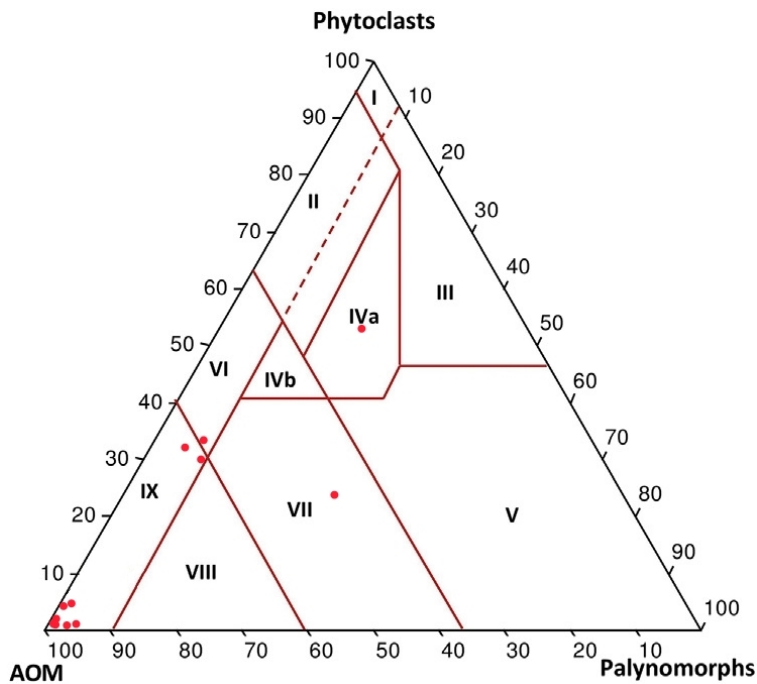


**Figure 22:** APP plots for the 13 kerogen slides from core 7831/2-U-1, showing a dominance of AOM with an increasing input of terrestrial organic matter. The fields corresponds to the environment explanation in Figure 20 (after Tyson, 1995).

phytoclasts amounted to a total of 31 and 26 percent, respectively. The palynomorphs consisted mostly of sporomorphs, but phytoplankton also occurred. The phytoclasts comprised mainly of oxidized or carbonized woody tissues (16 percent), but wood tracheid tissues without pits was also common (seven percent). Some “membranes”, “pseudo-amorphous” phytoclasts, cuticles and wood tracheid tissue without visible pits also occurred. Thus, the sample plotted in field VII (distal dysoxic-anoxic “shelf”, Fig. 22).

Overall, bisaccate pollen constituted most of the palynomorphs present in the kerogen slides, whereas spores and phytoplankton such as algae and the acritarch *Micrhystridium* spp. was rare. The phytoclasts comprised of opaque oxidized or carbonized woody tissue and wood tracheid tissue without biostructures (pits). Rare cuticles, “membranes”, fibrous bundles and wood tracheids with biostructures occur sporadically. The two latter only in the uppermost sample.

## 5. Discussion

### 5.1 Palynostratigraphy and age determination

Xu et al. (2014) have previously dated the two cores 7831/2-U-2 and 7831/2-U-1 based on Re-Os geochemistry. Three intervals in core 7831/2-U-2 and two intervals in core 7831/2-U-1 were sampled for the Re-Os datings (Xu et al., 2014, Appendix II). Three of these samples yielded isochron ages constraining the Ladinian - Carnian boundary within the cores (Appendices II and III). The boundary was constrained to the interval between 11.30 meter in core 7831/2-U-2 until 20.46 meter in core 7831/2-U-1. This places the stage boundary between 233.2 and 238.1 Ma, with a nominal age of 236.2 to 237.5 Ma (Xu et al., 2014), as according to Ogg (2012) is established at 237 Ma for the stage boundary. However, the one sample constraining the boundary within core 7831/2-U-1 is associated with large uncertainties (Appendices II and III). Xu et al. (2014) proposed the Ladinian-Carnian boundary to be within the underlying core 7831/2-U-2, thus consequently suggesting an earliest Carnian age for core 7831/2-U-1.

Vigran et al. (2014) tentatively assigned the lowermost part of core 7831/2-U-2 (18.85 to 14.89 meter) to their Ladinian age *Echinitosporites iliacooides* CAz, defined on the basis of the distinctive taxon *E. iliacooides*. Although they did not record *E. iliacooides* within this interval, only from 11.43 and 9.85 meter. Their assignment was based on the general characteristics of the association and the absence of *Aulisporites astigmosus*. In order to get a more detailed understanding, six additional samples (to their 12) were included in the present study. Interestingly enough two of these additional samples (16.75 and 12.64 meter) yield rare *E. iliacooides*, thereby extending the recorded range of the taxon in the core. The *E. iliacooides* CAz might therefore range up until 12.64 meter of core 7831/2-U-2, based on presence of the nominate taxon *E. iliacooides* and the same general characteristics of the association. The species is regarded as a marker for the Ladinian in the Germanic and Alpine realms (Visscher and Brugman, 1981), and thus originally thought to be restricted to the Ladinian also in the Boreal realm. However, this species is recorded in ammonite dated early Carnian beds on Bjørnøya (Mørk et al., 1990). The globular internal whorls of the ammonite *Nathorstites* sp.

obtained from 12.32 – 12.27 meter within core 7831/2-U-2 is indicative of *Nathorstites mclearni* of late Ladinian age (Xu et al., 2014). This is consistent with the palynological and Re-Os data for the lower part of the core.

Additional pollen species with their FADs in the lower part of the *Echinosporites iliacooides* CAz of Vigran et al. (2014) include *Schizaeosporites worsleyi*, *Triadispora verrucata*, *Staurosaccites quadrifidus* and *Ovalipollis pseudoalatus*. *Protodiploxypinus ornatus* occurs consistently throughout the zone. In the present study, *P. ornatus* and *S. worsleyi* occur mostly consistent throughout core 7831/2-U-2. *Triadispora verrucata* shows an increase in relative abundance from the base up until 12.64 meter, before decreasing again upwards. *S. quadrifidus* is present throughout. Vigran et al. (2014) reported *O. pseudoalatus* to be present in the upper part of the core (upwards from 11.43 meter), but relatively rare. In the present study, *O. pseudoalatus* is recorded (as *Ovalipollis* spp.) more frequently, with first occurrence in sample 16.75 meter. The monosulcate pollen *Chasmatosporites* spp. and *Chasmatosporites hians* are recorded sporadic throughout the core, together with rare *Cycadopites* spp. Monosaccoid pollen are characteristic for the *Echinosporites iliacooides* CAz (Vigran et al., 2014)

The Re-Os datings by Xu et al. (2014) suggest a correlation to assemblage H of Hochuli et al. (1989) for the palynological association recorded from the lower part of core 7831/2-U-2 (Fig. 24). However, several of the species recorded in the present study have their FADs in assemblage I of Hochuli et al. (1989). As these are long-ranging taxa, only six species separate assemblage I from assemblage H (Hochuli et al., 1989). These are *Annulispora* spp., *Jugasporites* spp., fungal remain type 1 (sensu Hochuli et al., 1989), *Angustisulcites grandis*, *Dyupetalum vicentinense* and the characteristic *Cordaitina gunyalensis*. With the exception of *Annulispora* spp., they all have their LADs in assemblage I (Hochuli et al., 1989). The fact that all of these species are unrecorded in the present study, might support correlation to assemblage H of Hochuli et al. (1989) for the lower part of core 7831/2-U-2 (Fig. 25).

The palynological association recorded from core 7831/2-U-2, shows similarities to an assemblage recorded from Bjørnøya by Mørk et al. (1990). Their recorded assemblage was correlated to assemblage G of Hochuli et al. (1989). However, Mørk et al. (1990) expressed

some uncertainty regarding this assignment. Vigran et al. (2014) reassigned the association recorded by Mørk et al. (1990) to assemblage I of Hochuli et al. (1989, Fig. 25), consequently suggesting an absence of assemblage H (Hochuli et al., 1989) on Bjørnøya (Fig. 25). However, only one of the six species separating assemblage H from assemblage I is recorded by Mørk et al. (1990). This included one sample yielding rare *Cordaitina gunyalesis*, occurring in the *Echinitosporites iliacooides* CAz of Vigran et al. (2014) but not ranging into younger strata. This taxon has also its LAD in assemblage I (Hochuli et al., 1989). Thus, the assignment to assemblage H (Hochuli et al., 1989) was possibly conducted based on this occurrence.

There are several distinct differences between the recorded assemblage in the present study and that of Mørk et al. (1990), these include common occurrences of *Alisporites* spp., *Staurosaccites quadrifidus*, *Ovalipollis* spp., *Triadispora verrucata* and *Schizaeosporites worsleyi* in the present study. *Camarozonosporites rudis* and *Calamospora tener* have sporadic occurrences near the top in both assemblages. Overall, the palynological association in the present study is much more consistent throughout, than in the assemblage recorded by Mørk et al. (1990) on Bjørnøya. However, the succession on Bjørnøya is much thicker and holds a higher sampling density.

Hochuli et al. (1989) recorded the FADs of the stratigraphically important *Camarozonosporites rudis* and *Camarozonosporites laevigatus* in their assemblage G. In the present study, these occur upwards from 10.28 and 9.30 meter in core 7831/2-U-2, respectively. This is consistent with an assemblage G association for the upper part and an assemblage H association for the lower part in core 7831/2-U-2 (Fig. 25), as expected from the Re-Os datings by Xu et al. (2014). Hochuli et al. (1989) had originally placed the Ladinian – Carnian boundary between their assemblages G and F. This assignment was probably a consequence of their records of *Echinitosporites iliacooides*, which at the time were thought to be restricted to the Ladinian.

Because of uncertainties regarding the Re-Os isochron ages, Xu et al. (2014) reviewed the palynological data provided by Vigran et al. (2014), to supplement the stage boundary determination. They concluded that the palynological assemblages from the two cores were equivocal, not permitting a confident or any more precise determination of the Ladinian - Carnian boundary. Xu et al. (2014) stated that based on palynology, the Ladinian - Carnian

boundary could be somewhere within the interval above 11.43 meter in core 7831/2-U-2 until 19.66 meter in the overlying core 7831/2-U-1. Thus, the interval containing the Ladinian - Carnian boundary within the two cores spans an interval of 13.79 meter based on palynology. In addition, the possible stratigraphic gap between the cores, estimated as up to 30 meter (Riis et al., 2008), increases the uncertainty (Figs. 23a – 25).

In the Svalbard and Barents Sea area, the Ladinian – Carnian boundary has been identified by a gradual shift in the palynological associations (Vigran et al., 2014). Thus, the Re-Os datings by Xu et al. (2014) offered a unique opportunity to investigate whether this is the case in the studied area. Vigran et al. (2014) had previously carried out a preliminary study of samples from cores 7831/2-U-2 and 7831/2-U-1. The present study thereby provides for the first time semi-quantitative counts from this area. Three intervals in core 7831/2-U-2 were sampled for Re-Os dating (Xu et al., 2014). Two of these samples, from the upper part of the core, yielded isochron ages consistent with the established stage boundary age. The two isochron ages have relatively small uncertainties and constrain the Ladinian – Carnian boundary relatively closely (Appendix II). The two samples were collected from 11.30 – 11.12 meter and 10.34 – 10.18 meter (Appendix II).

In Svalbard, the Ladinian - Carnian boundary coincides approximately with the contact between the Sassendalen and Kapp Toscana groups, with the exception of Bjørnøya (Xu et al., 2014, Figs. 7 and 23b), as the group boundary is considered diachronous across the region (Riis et al., 2008; Weitschat and Dagys, 1989, Figs. 7 and 23b). In the study area, east offshore Kong Karls Land, the Ladinian – Carnian stage boundary might not coincide entirely with this group boundary (Xu et al., 2014, Fig. 23b).

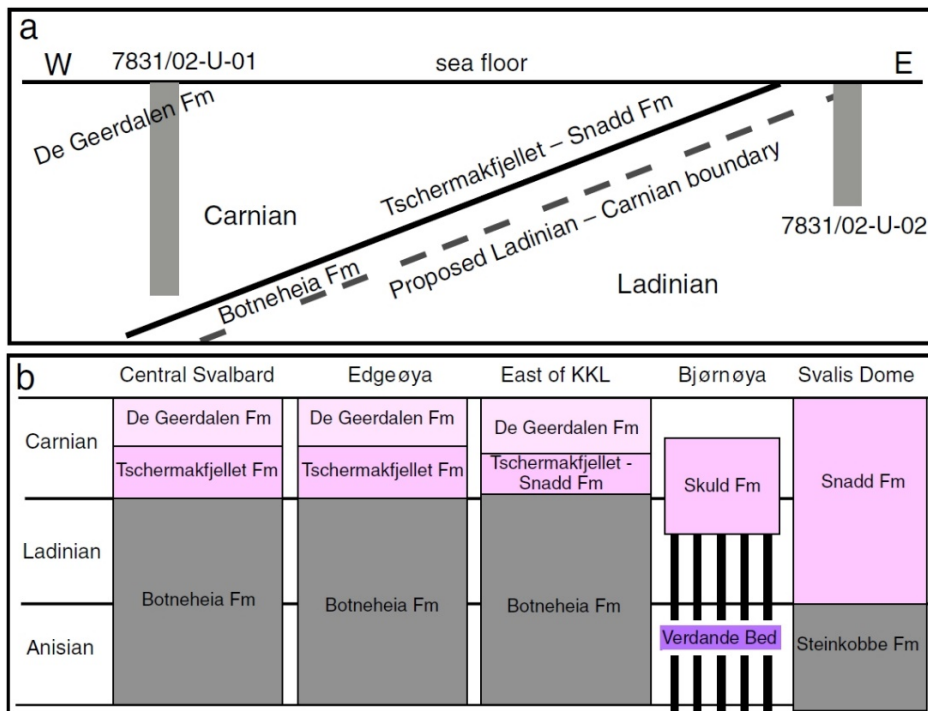


**Figure 23:** a) Proposed Ladinian - Carnian boundary by Xu et al. (2014) within the two studied cores. Note that the Ladinian - Carnian boundary does not coincide with the formational boundary between the Botneheia and Tschermakfjellet formations (from Xu et al., 2014). b) Stratigraphic scheme, showing the Botneheia Formation slightly ranging into the Carnian in the study area, east of Kong Karls Land (KKL) (from Xu et al., 2014).

Riis et al. (2008) placed the formational boundary between the Botneheia and the Tschermakfjellet formations within the possible gap between the two cores (Fig. 26). However, the cores do represent a depositional continuity (Lundschieen et al., 2014, Fig. 26). The two cores show that the lithological change between the Botneheia and the Tschermakfjellet formations is more gradual than between the formations on Edgeøya (Riis et al., 2008). Xu et al. (2014) discussed the lithological change upwards from 19 meter in core 7831/2-U-1. No chert nor phosphate nodules were observed in this interval, which is essentially lacking within the Tschermakfjellet Formation (Mørk et al., 1999). Therefore, they suggested this gradual shift in the lower interval from 27.95 until 19 meter to be indicative of the transition from the phosphate- and chert- bearing Botneheia Formation to the Tschermakfjellet Formation (Xu et al., 2014). In central Spitsbergen and eastern Svalbard, the lower boundary of the Tschermakfjellet Formation is defined where gray, silt- bearing shale with red, weathering siderite nodules and laminae occur above the darker, more organic rich and cliff- forming Blanknuten Member (Mørk et al., 1999, Fig. 17c). Sparse siderite nodules

and laminae, and abundant pyrite make the shale interval from 19 until 14 meter in core 7831/2-U-1 resemble the Tschermakfjellet Formation on Edgeøya (Xu et al., 2014). Core 7831/2-U-2 and the shales from the lower interval of core 7831/2-U-1 show major facies differences compared to the correlative cored interval in the Sentralbanken High area (Høy and Lundschieen, 2011).

The cores have previously been correlated to core 7534/4-U-1 from the Sentralbanken High area by Riis et al. (2008) and Lundschieen et al. (2014). Landa (2015) recently studied this core for palynology and palynofacies. The palynological assemblages recorded in the present study show several significant differences compared to the assemblage from the correlative interval of core 7534/4-U-1. In core 7534/4-U-1, the Ladinian – Carnian boundary coincides with an erosional surface, which hampers confident correlation to the distal cores in the present study.

In the present study, *Aulisporites astigmosus* is recorded sporadically upwards from 16.75 meter in core 7831/2-U-2. However, the records of *A. astigmosus* are somewhat uncertain in this core, as the diagnostic trilete mark is not observed. Vigran et al. (2014) recorded the first occurrence (FO) of *A. astigmosus* from 14.32 meter and used this to assign the interval above to their *A. astigmosus* CAz. This zone is essentially of Carnian age, but Vigran et al. (2014) tentatively assigned the lowermost part of core 7831/2-U-2 (14.32 to 13.88 meter) a Ladinian age. The recent Re-Os datings by Xu et al. (2014) also support a late Ladinian age for this interval. Since identification of *A. astigmosus* is uncertain, this remains an unsolved issue and should be worked on in a taxonomic study in the future. Vigran et al. (2014) assigned the upper interval of core 7831/2-U-2 (11.43 to 6.16 meter) a late Ladinian to early Carnian age. The Re-Os datings by Xu et al. (2014) support an early Carnian age for this part. The earliest occurrence of *A. astigmosus* within the Barents Sea might therefore be in the Ladinian.



Age	Palynological composite assemblage zones	Formations			Palynozonation					
		Svalbard		Barents Sea	Hochuli et. al. 1989	This study (7831/2-)	Mørk et al. 1990	Vigran et. al. 1998		
		West	East							
TRIASSIC	Late	Rhaetian	R. tuberculatus	Knorring-fjellet Fm	Flatsalen	Fruholmen	A			
		Norian	L. lundbladii				B			
		Late Carnian	Rhaetogonyaulax spp.	De Geerdalen	C					
		Middle Carnian	A. astigosus		D					
		Early Carnian			E					
	Middle	Ladinian	E. iliacoides	Bravaisberget	Botneheia	Snadd	F	I	I	S-8
							G			
		Late Anisian	P. decus	Steinkobbe Kobbe	K	S-7				
		Middle Anisian	T. obscura		L		S-6			
		Early Anisian	A. spiniger	S-5						

**Figure 24:** Correlation of the present study with the palynological composite assemblage zones of Vigran et al. (2014), and the works of Vigran et al. (1998), Mørk et al. (1990) and Hochuli et al. (1989). The stratigraphic thicknesses of cores 7831/2-U-2 and 7831/2-U-1 are not to scale (modified from Vigran et al., 2014).

Vigran et al. (2014) noted a general increase in the abundances of trilete and monoete spores in the Carnian Barents Sea succession, compared to the Ladinian. Such increases are recorded in the upper part of core 7831/2-U-2, with the FADs of trilete spores including the cavate *Kraeuselisporites* spp., the apiculate *Conbaculatisporites* spp., the laevigate spores *Calamospora tener* and *Dictyophyllidites mortonii* and the monoete spore *Aratrisporites* spp.

at 11.43 meter. The trilete murornate spore *Camarozonosporites rudis*, typical within the Carnian (Vigran et al., 2014) has its FAD at 10.28 meter. Other trilete spores with FADs at or near the top of the core includes the laevigate spore *Punctatisporites* spp., the murornate *Camarozonotriletes laevigatus* and *Lycopodiacidites* spp. and the azonate apiculate *Converrucosisporites* sp. A, the laevigate *Todisporites major*, the cavate *Kraeuselisporites cooksonae* and *Kraeuselisporites apiculatus* and the cavate monolete spore *Aratrisporites saturnii*. These taxa become increasingly common throughout the Carnian in the Barents Sea area (Vigran et al., 2014; Paterson and Mangerud, 2015).

In the youngest core 7831/2-U-1, the palynological association show a significant shift upwards. The lower interval (27.95 until 14.45 meter) is dominated by marine palynomorphs, with regular peaks of the acritarch *Micrhystridium* spp. In the upper interval (from 14.14 until 8.05 meter), marine palynomorphs are rare. This is consistent with marine palynomorphs occurring more episodically in the Late Triassic successions, than in Early and Middle Triassic successions in the Barents Sea area, as documented by Vigran et al. (2014). The increase of trilete and monolete spores in Carnian successions documented by Vigran et al. (2014) continues upwards in core 7831/2-U-1. In ascending order, this includes *Kyrtomispuris speciosis*, *Apiculatisporites lativerrucosus*, *Aratrisporites macrocavatus*, *Kraeuselisporites dentatus*, *Apiculatasporites hirsutus*, *Trachysporites asper*, *Limatulasporites limatulus*, *Apiculatisporites parvispinosus*, *Carnisporites spiniger*, *Aratrisporites laevigatus*, *Kyrtomispuris gracilis*, *Ischyosporites* spp., *Zebrasporites fimbriatus*, *Porcellispora longdonensis* and *Neoraistrickia taylorii*.

In the uppermost sample (8.05 meter), trilete spores with FADs include *Densosporites fissus*, *Lophotriletes novicus*, *Conbaculatisporites hopensis* and *Lycopodiumsporites semimuris*. The monolete spores *Aratrisporites paenulatus* and *Aratrisporites fimbriatus* also have their FADs in this sample. According to Vigran et al. (2014), cavate trilete spores are rare in the Ladinian and Carnian successions. However, there are exceptions, as various *Krauselisporites* species can be common in certain intervals, especially in early Carnian successions (e.g. Hochuli and Vigran, 2010). Diverse species of the cavate trilete *Krauselisporites* group are recorded sporadic throughout core 7831/2-U-1. In addition, trilete smooth spores including *Calamospora tener* and *Punctatisporites* spp. are partly common. *Dictyophyllidites mortoni*

and *Deltoidospora* spp. show a general increase in relative abundance upwards from 14.45 meter until the uppermost sample from 8.05 meter.

Rare to abundant occurrences of species of the *Ovalipollis*, *Protodiploxypinus*, *Chasmatosporites* and *Araucariacites* groups, and *Aulisporites astigmosus* are recorded throughout core 7831/2-U-1. The three latter are generally increasing in abundance upwards. With the exception of the *Protodiploxypinus* group, they all show a relative increase in abundance compared to within the Ladinian age assemblage from the underlying core 7831/2-U-2. The *Protodiploxypinus* group has common to abundant occurrences in both cores, and shows no significant change in abundance between the two. It is interesting to note that Hochuli and Vigran (2010) and Vigran et al. (2014) documented increases in the abundance of certain gymnosperm pollen in Carnian successions compared to successions of Ladinian age.

Vigran et al. (2014) have previously assigned core 7831/2-U-1 to their *Aulisporites astigmosus* CAz based on common to dominant *Aulisporites astigmosus* and the general characteristics of the association, containing many stratigraphically younger taxa compared to the older *Echinitosporites iliacooides* CAz. However, they tentatively assigned the lowermost interval (26.61 to 24.36 meter) a Ladinian/Carnian age and the uppermost interval (14.83 to 11.85 meter) an early Carnian age. A sample from 19.66 meter was not assigned any age. Their study of the core was carried out by examination of five palynological samples, whereas 13 additional samples were available for the present study. Vigran et al. (2014) noted that Carnian palynomorphs generally are better preserved than those of Ladinian age, and this is also the case herein. This might have to do with the fact that during the Ladinian, the Svalbard area was situated in a shallow marine to deep shelf setting (Fig. 5b) leaving the sporomorphs prone to oxidation and degradation during their offshore transport. Pyrite crystallisation is also responsible for degrading the palynomorphs.

The Re-Os datings by Xu et al. (2014) suggest correlation to the assemblage G of Hochuli et al. (1989). Twenty-five of 37 species recorded by Hochuli et al. (1989) in their assemblage G are recorded from core 7831/2-U-1. Nevertheless, the palynological association recorded in the present study seems to correlate somewhat better with assemblage F, due to the presence of *Aulisporites astigmosus*, *Chasmatosporites* spp. and *Aratrisporites* spp., which have their FADs

in the assemblage (Hochuli et al., 1989). However, as mentioned earlier, Mørk et al. (1990) recorded the two latter taxa from strata of Ladinian age on Bjørnøya. Seven species separates assemblage G from assemblage F. Two of these have their FADs in assemblage F (Hochuli et al., 1989) and they are not observed in the present study nor by Vigran et al. (2014). The remaining two species separating the two assemblages are *Echinosporites iliacoides* and *Retisulcites perforatus*. These have their LADs in assemblage G (Hochuli et al., 1989). In the present study, a single specimen of *E. iliacoides* was observed in the sample from 22.83 meter. Vigran et al. (2014) recorded the taxon from the samples from 26.61 and 24.33 meter, in addition to common *Retisulcites perforatus* from sample 11.85 meter.

Hochuli et al. (1989) recorded the FO of *Aulisporites astigosus* within their assemblage F (Fig. 24). However, *A. astigosus* has previously been recorded from Ladinian successions elsewhere in the world (e.g. Hankel, 1993; Geleta and Wille, 1998; Brugman et al., 2004; Kürschner and Herengreen, 2010).

Vigran et al. (2014) documented a relative decrease in the diversity of taeniatae bisaccate pollen in Carnian age palynological associations compared to Ladinian age associations. Such a decrease was also observed by Kürschner and Herengreen (2010) in associations from central and northwestern Europe, and might have been caused by different climatic factors (Vigran et al., 2014). In the present study, a minor decrease in the diversity of bisaccate taeniatae pollen is recorded between the two cores. This decrease is shown as *Protohaploxylinus* spp. and *Striatoabieites aytugi* only occur in core 7831/2-U-2.

The Ladinian and early Carnian age assemblages of Hochuli et al. (1989) differ considerably from palynological assemblages spanning the Ladinian - Carnian boundary in the southern part of the Russian Barents Sea (Mørk et al., 1992). In the Russian Arctic, the palynoflora from this interval is dominated by *Cycadopites* spp. and maximums of *Echinosporites iliacoides* and *Illinites* spp. In addition, *Schizaeoisporites worsleyi* is restricted to this interval (Mørk et al., 1992). This indicates that the western Barents Sea area and the southern Russian area represented different floral provinces (Mørk et al., 1992).

As expected, no dinoflagellate cysts were recorded in the present study. There are no published records of dinocysts within the early Carnian in the Svalbard and Barents Sea area (oral communication; Paterson, 2015). The earliest records of dinocysts in the area are not until the late Carnian (Paterson and Mangerud, 2015), and generally their first common occurrence is in the Norian Flatsalen Formation.

## 5.2 Palaeoenvironments

The Botneheia Formation represented in core 7831/2-U-2 was deposited as part of the bottom sets of the major delta, prograding from the southeast towards the northwest on the Barents Sea Shelf (Høy and Lundschieen, 2011). According to Høy and Lundschieen (2011), turbidites occurred sporadically, reflected in core 7831/2-U-2 by pro-delta deposits of laminated dark shale (Figs. 14 and 15a) with sporadic and thin, weathering carbonaceous siltstone layers (Fig. 15a). The palynological samples from core 7831/2-U-2 yield abundant marine palynomorphs, together with bisaccate pollen (Fig. 12 and Appendix III). The high abundance of bisaccate pollen can be explained by the Neves effect (Chaloner and Muir, 1968), explaining why palynological assemblages from deep marine environments often show relative enrichments of bisaccate, hinterland pollen. Due to the fact that saccates are easily transported over long distances by air and water, before settling in quiet environments. Hence, these parts of the assemblage are rather indicative of an upland flora, and not an indication of the flora being in near proximity to the basin margins (Traverse, 2007). Bivalves occur sporadically in core 7831/2-U-2, and rare ammonites have previously been obtained (Xu et al., 2014).

The high organic content in core 7831/2-U-2 indicates deposition within a restricted, deep shelf setting with anoxic bottom water conditions (Lundschieen et al., 2014). The palynofacies analysis from core 7831/2-U-2 (the Botneheia Formation) and the lower part of core 7831/2-U-1 (up to 16.25 meter, which represents a gradual shift from Botneheia Formation to the Tschermakfjellet Formation) revealed a dominance of AOM as illustrated in the ternary plots (Figs. 21 and 23). This is indicative of deposition within a distal suboxic-anoxic environment

(Tyson, 1995). Pyrite inclusions are observed in the AOM, which is typical for AOM of highly reducing environments (Tyson, 1995). Anoxic bottom water (deep water deficient in oxygen) can be a result of restricted circulation and varying density of water bodies, causing density stratification within the water column (Streef, 1999). The high abundance of phosphate in the cores, indicate high content of phosphate in the seawater (Nystuen et al., 2007). During the Triassic, rivers coming from Siberia and the Caledonides supplied the Panthalassa Ocean with sediments, phosphate, nutrients and fresh water (Høy and Lundschieen, 2011). Høy and Lundschieen (2011) proposed a hypothesis that this fresh water lead to a chemocline in the ocean (Fig. 27), resulting from density differences between the fresh water and the saline seawater. Their hypothesis is that this played a more important role in the generation of the anoxic bottom water conditions, than subsidence of the sea floor.

Høy and Lundschieen (2011) proposed that the rock-forming algae *Tasmanites* spp. observed between 14.35 and 15.55 meter in core 7831/2-U-2 (Figs. 14c and 16a), played an important role in algal blooms in front of the prograding Carnian delta. According to their hypothesis, river-transported nutrients gave rise to such massive blooms. This caused massive death zones in front of the delta, as microbial organisms would exhaust the oxygen in the water masses during the digestion process of the algae. This may explain the lack of bioturbation in core 7831/2-U-2. Several authors have documented similar intervals of dominating *Tasmanites* (Figs. 14c, 16a-b) from the Botneheia Formation (e.g. Krajewski, 2008; Vigran et al., 2008; Mørk and Bromley, 2008; Krajewski, 2013).

Core 7831/2-U-2 differs from the Botneheia Formation on Edgeøya (Fig. 15c) by the presence of the chert nodules (Fig. 14a) which are interpreted by Riis et al. (2008) to possibly be derived from skeletal material of siliceous sponges. According to Riis et al. (2008), this might indicate a more distal and deeper depositional environment for core 7831/2-U-2, than for the Botneheia Formation on Edgeøya.

Based on the height of the prograding clinoforms, Lundschieen et al. (2014) interpreted the seawater depth to be up to 400 meter in the area during the Ladinian (Fig. 25). Tyson (1987) expressed the importance of bathymetric factors in the control of Total Organic Carbon content (TOC).

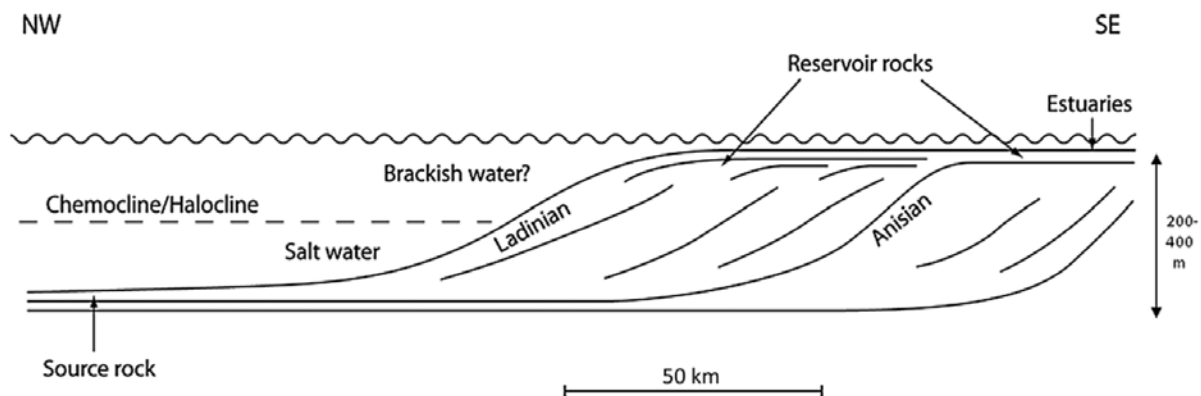


**Figure 25:** General environmental conditions in the northern Barents Sea during the Ladinian. The Botneheia Formation was deposited in a distal, deep shelfal setting, as the bottom sets of a prograding delta (from Høy and Lundschieen, 2011).

From the Tschermakfjellet Formation, in the upper part of core 7831/2-U-1 (from 14.45 meter), an increase of phytoclasts is observed. In addition, an upwards increase of spores and a decrease of marine palynomorphs are recorded, this corresponds with the pronounced change in the lithofacies. This is consistent with the delta reaching the Kong Karls Land area in the early Carnian, as documented by several authors (e.g. Riis et al., 2008; Høy and Lundschieen, 2011). However, the ratio between the AOM, palynomorphs and phytoclasts vary in this upper part, probably indicating periods of fluctuating restriction within the depositional environment. This is in agreement with geochemical analyses, which show a low organic content in core 7831/2-U-1 suggesting more oxic conditions (Riis et al., 2008). Riis et al. (2008) interpreted the two cores to have been deposited in a more distally offshore setting than the Tschermakfjellet Formation and the uppermost part of the Botneheia Formation on Edgeøya.

In terms of the marine palynomorphs, regular acmes of acritarchs occur in the lower part of core 7831/2-U-1 (Appendix IV), indicative of a fully marine environment. The acritarch *Micrhystridium* spp. occurs in restricted shallow marine environments, whereas *Veryhachium* spp. occurs in open, shallow marine environments (Ercegovac and Kostić, 2006). The varying abundances of these two genera in core 7831/2-U-2 and 7831/2-U-1 (Appendices IV and V) might thus reflect changes in the restriction of the depositional environment. The fresh water algae *Botryococcus* spp. occurs sporadic in both cores. This indicates periods of fresh water input, causing brackish surface water conditions (Bremer et al., 2004, Fig. 25). In sample 10.28

meter from core 7831/2-U-2, a significant increase of bisaccate pollen, coupled with a significant decrease of marine palynomorphs is recorded. Streel and Richelot (1994) proposed that flood events could be the main reason for such occurrences, transporting pollen to deep marine environments.

The Tschermakfjellet Formation in the uppermost interval in core 7831/2-U-1 (from 13.25 until 8.00 meter) contains silt- and sandstones with sporadic coal fragments (Fig. 19b), typical for the Snadd Formation in the Barents Sea (Lundschien et al., 2014). This indicates a more proximal shelf setting during the deposition of this interval, with coal swamps in near proximity to the prograding delta. Core 7831/2-U-1 also shows an upwards increase of *Araucariacites* spp. from 14.45 meter, coupled with sporadic *Cycadopites* spp. Hochuli and Vigran (2010) reported an increase of *Araucariacites* and cycadophytes from Upper Triassic strata from the Barents Sea area. They interpreted these increases as indicative of a climatic change in the region.



## 6. Conclusions

The Ladinian – Carnian boundary in the Svalbard and Barents Sea area can usually be observed as a gradual shift in the palynological assemblages. The Re-Os datings by Xu et al. (2014) offered a unique opportunity to investigate whether this is also the case in the studied area offshore Kong Karls Land.

The palynological samples from core 7831/2-U-2 yielded poorly preserved palynomorphs, mainly bisaccate pollen, algae and acritarchs, indicative of a marine depositional environment, consistent with the laminated shale in the core. The palynofacies analysis revealed a dominance of AOM, indicative of anoxia, consistent with the lack of bioturbation.

The palynological assemblages recorded from the oldest core 7831/2-U-2 are assigned to the *Echinosporites iliacooides* Composite Assemblage zone (CAz) and the *Aulisporites astigosus* CAz of Vigran et al. (2014). The ammonite *Nathorstites mclearnii* of late Ladinian age has previously been obtained from the lower part of the core, supporting the age for this part of the core.

The youngest core 7831/2-U-1 is assigned to the *Aulisporites astigosus* CAz of Vigran et al. (2014).

The youngest core 7831/2-U-1 shows an upwards increase of trilete spores typical within the Carnian, coupled with a decrease in marine palynomorphs. This corresponds with an increasingly proximal lithofacies upwards in the core, with silt- and sandstone in the upper part. The upper part also contains coal fragments. The lower interval shows peaks of the acritarch *Micrhystridium* spp., suggesting a fully marine environment for this interval.

The palynofacies analysis of core 7831/2-U-1 shows a dominance of AOM in the lower interval, fluctuating upwards from 14.45 meter, with a coupled increase in terrestrial kerogen. This is consistent with the lithofacies and palynological data, and suggests the arrival of the prograding, early Carnian delta in the Kong Karls Land area.

The integrated lithofacies, palynofacies analyses and palynological data indicate a more distal environment than recorded elsewhere in the region.

The present study shows that the transition in palynological assemblages across the inferred Ladinian – Carnian boundary is gradual in studied area. Therefore, it may not be possible to recognize the Ladinian – Carnian boundary based on palynology alone.

## References

- Abbink, O. A., 1998. Palynological investigations in the Jurassic of the North Sea region. *Lab. Palaeobot. Palynol. Contrib. Ser.*, 8, 1-191
- Armstrong, H. A., & Brasier, M. D., 2005. Spores and Pollen. *Microfossils, Second Edition*, 104-125. Blackwell Publishing.
- Ask, M., 2013. Palynological dating of the upper part of the De Geerdalen Formation on central parts of Spitsbergen and Hopen (MSc. thesis), University of Bergen, Norway, 1-79.
- Bagatikov, O. A., Kovalenko, V. I., & Sharkov, E. V., 2000. General features of magmatic evolution throughout the Earth's history. In O. A. Bagatikov (Ed.), *Magmatism and Geodynamics: Terrestrial Magmatism Throughout the Earth's History*, p. 353. Gordon & Breach Science Publ., Amsterdam.
- Batten, D. J., & Stead, D. T., 2005. Palynofacies analysis and its stratigraphic application. In *Applied Stratigraphy*, 203-226. Springer, Netherlands.
- Bjærke, T., 1977. Mesozoic palynology of Svalbard II. Palynomorphs from the Mesozoic sequence of Kong Karls Land. *Norsk Polarinstitutt Årbok 1976*, 83-120.
- Bjærke, T., & Manum, S. B., 1977. Mesozoic palynology of Svalbard. I, The Rhaetian of Hopen, with a preliminary report on the Rhaetian and Jurassic of Kong Karls Land. *Norsk Polarinstitutt*, no. *Skrifter nr. 135*, 1-48.
- Blendinger, E., 1988. Palynostratigraphy of the late Ladinian and Carnian in the southeastern Dolomites. *Review of palaeobotany and palynology*, 53, 329-348.
- Bremer, G. M. A., Smelror, M., Nagy, J., & Vigran, J. O., 2004. Biotic responses to the Mjølnir meteorite impact, Barents Sea: evidence from a core drilled within the crater. In H. Dypvik, M. Burchell, & P. Claeys (Eds.), *Cratering in marine environments and on ice*, 21-38. Springer, Berlin.
- Cirilli, S., 2010, Upper Triassic–lowermost Jurassic palynology and palynostratigraphy: a review: *Geological Society, London, Special Publications*, 334(1), 285-314.
- Combaz, A. (1964). Les palynofacies. *Revue de Micropaléontologie*, 7(3), 205-218.
- Dagys, A. S., Weitschat, W., Konstantinov, A. G., & Sobolev, E. S., 1993. Evolution of the boreal marine biota and biostratigraphy at the Middle/Upper Triassic boundary. *Mitteilungen aus dem Geologisch-Paläontologischen Institut der Universität Hamburg*, (75), 193-209.
- Doherty, L. I., 1980. Palynomorph preparation procedures currently used in the paleontology and stratigraphy laboratories, *US Geological Survey*, 830. US Dept. of the Interior, Geological Survey, 1-29.
- Downie, C., 1967. The geological history of the microplankton. *Rev. Palaeobotan. Palynol.* 1, 269-281.
- Ercegovac, M., & Kostić, A., 2006. Organic facies and palynofacies: nomenclature, classification and applicability for petroleum source rock evaluation. *International Journal of Coal Geology*, 68(1), 70-78.
- Faleide, J. I., Tsikalas, F., Breivik, A. J., Mjelde, R., Ritzmann, O., Engen, O., ... & Eldholm, O., 2008. Structure and evolution of the continental margin off Norway and the Barents Sea. *Episodes*, 31(1), 82-91.
- Faleide, J. I., Gudlaugsson, S. T., and Jacquart, G., 1984, Evolution of the western Barents Sea. *Marine and Petroleum Geology*, 1(2), 123-150.
- Felix, C. J., 1975. Palynological evidence for Triassic sediments on Ellef Ringnes Island, Arctic Canada. *Review of Palaeobotany and Palynology*, 20(1), 109-117.

- Fisher, M. J., 1979. The Triassic palynofloral succession in the Canadian Arctic Archipelago. *American Association of Stratigraphic Palynologists Contribution Series 5B*, 83-100.
- Glørstad-Clark, E., Faleide, J. I., Lundschieen, B. A., & Nystuen, J. P., 2010. Triassic seismic sequence stratigraphy and paleogeography of the western Barents Sea area. *Marine and Petroleum Geology*, 27(7), 1448-1475.
- Hesse, M., Halbritter, H., Weber, M., Buchner, R., Frosch-Radivo, A., & Ulrich, S., 2009. *Pollen terminology: an illustrated handbook*. Springer Science & Business Media.
- Hochuli, P. A., Colin, J. P., & Vigran, J. O., 1989. Triassic biostratigraphy of the Barents Sea area. In J. Collinson, (Ed.), *Correlations in Hydrocarbon Exploration*, Graham and Trotman, London, pp. 131–153.
- Hochuli, P. A., Roghi, G., & Brack, P., 2014. Palynological zonation and particulate organic matter of the Middle Triassic of the Southern Alps (Seceda and Val Gola–Margon sections, Northern Italy). *Review of Palaeobotany and Palynology*.
- Hoffmeister, W. S., 1954. Microfossil prospecting for petroleum. U.S. Patent, 2, 686, 108, 4.
- Holen, L. H., 2014. Late Triassic (Carnian) Palynology of the Northern Barents Sea (Sentralbanken High). (MSc. thesis), University of Bergen, Norway, 1-96.
- Hyde, H. A., & Williams, D. A., 1944. The right word. *Pollen Analysis Circular*, 8(6).
- Høy, T., & Lundschieen, B. A., 2011. Triassic deltaic sequences in the northern Barents Sea. *Geological Society, London, Memoirs*, 35(1), 249-260.
- Klaus, W., 1960. Sporen der karnischen Stufe der ostalpinen Trias, *Jahrb. Geol. Bundesanst.*, 107–183.
- Klausen, T. G., & Mørk, A., 2014. The Upper Triassic paralic deposits of the De Geerdalen Formation on Hopen: Outcrop analog to the subsurface Snadd Formation in the Barents Sea. *AAPG Bulletin*, 98(10), 1911-1941.
- Krajewski, K. P., Karcz, P., Wozny, E., & Mørk, A., 2007. Type section of the Bravaisberget Formation (Middle Triassic) at Bravaisberget, western Nathorst Land, Spitsbergen, Svalbard. *Polish Polar Research*, 28(2), 79-122.
- Krajewski, K. P., 2013. Organic matter–apatite–pyrite relationships in the Botneheia Formation (Middle Triassic) of eastern Svalbard: Relevance to the formation of petroleum source rocks in the NW Barents Sea shelf. *Marine and Petroleum Geology*, 45, 69-105.
- Kürschner, W. M., & Herengreen, G. W., 2010. Triassic palynology of central and northwestern Europe: a review of palynofloral diversity patterns and biostratigraphic subdivisions. *Geological Society, London, Special Publications*, 334(1), 263-283.
- Lundschieen, B. A., Høy, T., & Mørk, A., 2014. Triassic hydrocarbon potential in the Northern Barents Sea; integrating Svalbard and stratigraphic core data. *Norwegian Petroleum Directorate Bulletin*, 11, 3-20.
- Mädler, K., 1963. Die figurierten organischen Bestandteile der Posidonien-schiefer. *Beih. Geol. Jb.*, 58, 287-407.
- Mädler, K., 1964. Die geologische Verbreitung von Sporen und Pollen in der deutschen Trias (Doctoral dissertation, Niedersächs. Landesanst. für Bodenforschung).
- Manten, A. A., 1967. Lennart von Post and the foundation of modern palynology. *Review of Palaeobotany and Palynology*, 1(1), 11-22.
- Martin, R. E., 1999. *Taphonomy: a process approach* (Vol. 4). Cambridge University Press.
- Mendonça Filho, J. G., da Silva, F. S., de Oliveira, A. D., de Oliveira Mendonça, J., Rondon, N. F., da Silva, T. F., & Menezes, T. R., 2012. Organic facies: palynofacies and organic geochemistry approaches. In D. Panagiotaras (ed.), *Geochemistry – Earth’s system processes*. InTech, Rijeka, pp. 211-248.

- Muller, J., 1959. Palynology of recent Orinoco delta and shelf sediments: reports of the Orinoco shelf expedition; volume 5. *Micropaleontology*, 1-32.
- Mueller, S., Veld, H., Nagy, J., & Kürschner, W. M., 2014. Depositional history of the Upper Triassic Kapp Toscana Group on Svalbard, Norway, inferred from palynofacies analysis and organic geochemistry. *Sedimentary Geology*, 310, 16-29.
- Mørk, A., & Worsley, D., 2006. Triassic of Svalbard and the Barents shelf. *Boreal Triassic*, 3, 23-29.
- Mørk, A., Dallmann, W. K., Dypvik, H., Johannessen, E. P., Larssen, G. B., Nagy, J., Nøttvedt, A., Olaussen, S., Pchelina, T. M., and Worsley, D., 1999. Mesozoic lithostratigraphy: *Lithostratigraphic lexicon of Svalbard*. Upper Palaeozoic to Quaternary bedrock. Review and recommendations for nomenclature use, p. 127-214.
- Mørk, A., Vigran, J. O., and Hochuli, P. A., 1990. Geology and palynology of the Triassic succession of Bjørnøya. *Polar Research*, 8(2), 144-168.
- Nystuen, J. P., 1989. Rules and recommendations for naming geological units in Norway, *Norw. J. Geol.*, 69 (suppl. 2).
- Nystuen, J. P., Mørk, A., Müller, R., Nøttvedt, A., 2008. From desert to alluvial plain – from land to sea. In I. B. Ramberg (Ed.), *The making of a land: geology of Norway*, Trondheim: Norwegian Geological Society, pp. 330-334, 346-353.
- Ogg, J. G., 2012. The Triassic Period. In F. M. Gradstein, G. Ogg, & M. Schmitz (Eds.), *The Geologic Time Scale 2012 2-Volume Set, Volume 2*. Elsevier, UK.
- Paterson, N. W., & Mangerud, G., 2015. Late Triassic (Carnian–Rhaetian) palynology of Hopen, Svalbard. *Review of Palaeobotany and Palynology*.
- Paterson, N. W., Mangerud, G., Cetean, C. G., Mørk, A., Lord, G. S., Klausen, T. G., & Mørkved, P. T., 2015. A multidisciplinary biofacies characterisation of the Late Triassic (late Carnian–Rhaetian) Kapp Toscana Group on Hopen, Arctic Norway. *Palaeogeography, Palaeoclimatology, Palaeoecology*.
- Paterson, N. W., Mangerud, G., B. A., Lundschieen & Mørk, A., (in prep.). Late Triassic (early Carnian) palynology of shallow stratigraphic core 7830/5-U-1, offshore Kong Karls Land, Norwegian Arctic.
- Pčelina, T. M., 1983. New data on the Mesozoic stratigraphy of the Spitsbergen Archipelago. In A. A. Krasilnikov and V.A. Basov (eds.), *Geology of Spitsbergen*. PGO Sevmorgeo, Leningrad, 121–141.
- Punt, W., Hoen, P. P., Blackmore, S., Nilsson, S., & Le Thomas, A., 2007. Glossary of pollen and spore terminology. *Review of Palaeobotany and Palynology*, 143(1), 1-81.
- Raevskaya, E. G., & Servais, T., 2009. Ninadiacrodium: A new Late Cambrian acritarch genus and index fossil. *Palynology*, 33(1), 219-239.
- Riding, J. B., & Kyffin-Hughes, J. E., 2004. A review of the laboratory preparation of palynomorphs with a description of an effective non-acid technique. *Revista Brasileira de Paleontologia*, 7(1), 13-44.
- Riding, J. B., & Kyffin-Hughes, J. E., 2011. A direct comparison of three palynological preparation techniques. *Review of Palaeobotany and Palynology*, 167(3), 212-221.
- Riis, F., Lundschieen, B. A., Høy, T., Mørk, A., and Mørk, M. B., 2008, Evolution of the Triassic shelf in the northern Barents Sea region. *Polar Research*, 27(3), 318-338.
- Sakshaug, E., Bjørge, A., Gulliksen, B., Loeng, H., & Mehlum, F., 1994. Structure, biomass distribution, and energetics of the pelagic ecosystem in the Barents Sea: a synopsis. *Polar Biology*, 14(6), p. 405.
- Smith, D. G., 1974. Late Triassic pollen and spores from the Kapp Toscana Formation,

- Hopen,  
Svalbard—a preliminary account. *Review of palaeobotany and palynology*, 17(1), 175-178.
- Smith, D. G., Harland, W. B., & Hughes, N. F., 1975. Geology of Hopen, Svalbard. *Geological Magazine*, 112(01), 1-23.
- Smith, D. G., 1982. Stratigraphic significance of a palynoflora from ammonoid-bearing Early Norian strata in Svalbard. *Newsletters on Stratigraphy*, 11(3), 154-161.
- Streel, M., & Richelot, C., 1994. Wind and water transport and sedimentation of miospores along two rivers subject to major floods and entering the Mediterranean Sea at Calvi (Corsica, France). *Sedimentation of organic particles*.
- Traverse, A., 2007. *Paleopalynology*. 2nd edition. Springer, Dordrecht, Netherlands, pp. 1-813.
- Tschudy, R. H., 1961. Palynomorphs as indicators of facies environments in Upper Cretaceous and Lower Tertiary strata, Colorado and Wyoming. Wyoming Geol. Assoc. *Guidebook 16*. Ann. Field Conference 53-59.
- Tyson, R. V., 1995. Palynological kerogen classification. In *Sedimentary Organic Matter*, pp. 341-365. Springer Netherlands.
- Van der Eem, J. G. L. A., 1983. Aspects of Middle and Late Triassic palynology. 6. Palynological investigations in the Ladinian and Lower Karnian of the western Dolomites, Italy. *Review of Palaeobotany and Palynology*, 39(3), 189-300.
- Vigran, J. O., Mangerud, G., Mørk, A., Bugge, T., & Weitschat, W., 1998. Biostratigraphy and sequence stratigraphy of the Lower and Middle Triassic deposits from the Svalis Dome, central Barents Sea, Norway. *Palynology*, 22, 89-141.
- Vigran, J. O., Mangerud, G., Mørk, A., Worsley, D., and Hochuli, P. A., 2014, Palynology and geology of the Triassic succession of Svalbard and the Barents Sea, *Geological Survey of Norway Special Publication*, 14, 247 pp.
- Visscher, H., & Brugman, W. A., 1981. Ranges of selected palynomorphs in the Alpine Triassic of Europe. *Review of Palaeobotany and Palynology*, 34(1), 115-128.
- Weitschat, W., & Dagys, A. S., 1989. Triassic biostratigraphy of Svalbard and a comparison with NE-Siberia. *Mitteilungen aus dem Geologisch-Paläontologischen Institut der Universität Hamburg*, 68, 179-213.
- Worsley, D., 2008, The post-Caledonian development of Svalbard and the western Barents Sea. *Polar Research*, 27(3), 298-317.
- Xu, G., Hannah, J. L., Stein, H. J., Mørk, A., Vigran, J. O., Bingen, B., Schutt, D. L., Lundschie, B. A., 2014. Cause of Upper Triassic climate crisis revealed by Re-Os geochemistry of Boreal black shales. *Palaeogeogr. Palaeoclimatol. Palaeoecol.* 395, 222-232.

## Appendices

- Appendix I: List of palynomorph taxa
- Appendix II: Re-Os datings of cores 7831/2-U-2 and 7831/2-U-1
- Appendix III: Range chart for core 7831/2-U-2
- Appendix IV: Plates 1- 6

## Appendix I: List of palynomorph taxa

### Spores

- Anapiculatisporites spiniger* (Leschik 1955) Reinhardt 1962  
*Apiculatasporites hirsutus* Leschik 1955  
*Apiculatisporites lativerrucosus* Leschik 1955  
*Apiculatisporites parvispinosus* (Leschik 1955) Playford & Dettman 1965  
*Aratrisporites fimbriatus* (Klaus 1960) Mädler 1964  
*Aratrisporites fischeri* (Klaus) Playford and Dettmann, 1965  
*Aratrisporites laevigatus* Bjærke & Manum 1977  
*Aratrisporites macrocavatus* Bjærke & Manum 1977  
*Aratrisporites paenulatus* Playford and Dettmann 1965  
*Aratrisporites saturnii* (Thiergart 1949) Playford and Dettmann 1965  
*Aratrisporites scabratus* Klaus 1960  
*Aratrisporites* spp.  
*Baculatisporites* spp.  
*Calamospora tener* (Leschik, 1955) Mädler 1964  
*Camarozonosporites laevigatus* Schulz 1967  
*Camarozonosporites rudis* (Leschik, 1955) Klaus 1960  
*Carnisporites spiniger*  
*Cingulizonates rhaeticus* (Reinhardt 1962) Schulz 1967  
*Clathroidites papulosus*  
*Conbaculatisporites hopensis* Bjærke & Manum 1977  
*Conbaculatisporites* spp.  
*Converrucosisporites* spp.  
*Deltoidospora* spp.  
*Densoisporites* spp. Dettmann, 1963  
*Densosporites fissus* (Reinhardt 1964) Schulz 1967  
*Densosporites* spp.  
*Dictyophyllidites mortonii* (de Jersey, 1959) Playford and Dettmann, 1965  
*Gordonispora* spp.



*Ischyosporites* spp.  
*Krauselisporites apiculatus* Jansonius 1962  
*Krauselisporites cooksonae* (Klaus 1962) Dettman 1963  
*Krauselisporites dentatus* Leschik 1956  
*Krauselisporites* spp.  
*Kyrtomispuris gracilis* Bjærke & Manum 1977  
*Kyrtomispuris laevigatus* Mädler 1964  
*Kyrtomispuris speciosis* Mädler 1964  
*Leschikisporis aduncus* (Leschik 1955) Potonié 1958  
*Limatulasporites limatulus* (Playford 1965) Helby & Foster 1979  
*Lophotriletes novicus* Singh 1964  
*Lycopodiacidites* spp.  
*Lycopodiumsporites semimuris* (Danze-Corsin and Laveine 1963) Mc Kellar 1974  
*Neoraistrickia taylorii* Playford and Dettmann 1965  
*Porcellispora longdonensis* (Clarke) Scheuring 1970 emend. Morbey 1975  
*Punctatisporites* spp.  
*Raistrickia* spp. Schopf, Wilson and Bentall, 1944  
*Retitriletes austroclavatidites* (Cookson 1953) Döring et al. 1963  
*Rogalskaisporites cicatricosus* Rogalska, 1954 ex Danze-Corsin and Laveine, 1963  
*Striatella parva* (Li and Shang) Filatoff and Price 1988  
*Striatella seebergensis* Mädler 1964  
*Thomsonisporites toralis* Leschik 1955  
*Tigrisporites halliensis* Klaus 1960  
*Todisporites major* Couper 1958  
*Todisporites minor* Couper 1958  
*Trachysporites asper*  
*Uvaesporites* spp.  
*Verrucosisporites* spp.  
*Zebrasporites fimbriatus* Klaus 1960

## Pollen

*Alisporites* spp.

*Angustisulcites klausii* (Freudenthal 1964) Visscher 1966

*Angustisulcites* spp.

*Araucariacites australis* Cookson 1947

*Aulisporites astigosus* (Leschik 1955) Klaus 1960

Bisaccate pollen

*Brachysaccus* spp.

*Chasmatosporites hians* Nilsson 1958

*Chasmatosporites* spp.

*Cycadopites* spp.

*Echinosporites iliacooides* Schulz 1961

*Granasporites magnus* Quian Lijun, Zao Cenghua and Wu Jinjun 1983

*Illinites chitonoides* Klaus 1964

*Instisporites crispus* Pautsch 1971

*Jerseyiaspora punctispinosa*

*Lunatisporites noviaulensis* (Leschik 1956) Scheuring 1970

*Ovalipollis* spp.

*Pinuspollenites* spp.

*Podosporites amicus* Scheuring 1970

*Protodiploxypinus decus* Scheuring 1970

*Protodiploxypinus macroverrucosus* Bjærke & Manum 1977

*Protodiploxypinus ornatus* (Pautsch 1973) Bjærke & Manum 1977

*Protodiploxypinus* spp.

*Protohaploxypinus* spp.

*Retisulcites* spp.

*Retisulcites* spp. A

*Schizaeoisporites worsleyi* Bjærke & Manum 1977

*Staurosaccites quadrifidus* Dolby and Balme 1976

*Striatoabieites aytugii* (Visscher 1966) Scheuring 1970

*Striatoabieites balmei* (Klaus 1964) Scheuring 1978

*Striatoabieites multistriatus* (Balme and Hennelly) Hart 1964

*Tetrasaccus* spp.

*Triadispora crassa* Klaus, 1964 Pl. 3, 3.

*Triadispora plicata* Klaus, 1964 Pl. 3, 2.

*Triadispora* ssp.

*Triadispora sulcate* Scheuring, 1978 Pl. 3, 4.

*Triadispora verrucata* (Schulz) Scheuring, 1970 Pl. 3,1.

*Vitreisporites pallidus* (Reissinger) Nilsson, 1958

### Acritarch

Acanthomorph acritarch

*Cymatiosphaera* spp.

*Micrhystridium* spp.

Sphaerical body (large)

Sphaeromorph cluster

*Veryhachium* spp.

### Chlorococcales

*Botryococcus* spp. Ktzing 1849

*Crassosphaera* spp.

*Leiosphaeridium* spp.

*Leiosphaeridium* spp. (large)

*Plaesiodictyon* spp.

*Pterospermella* spp.

*Tasmanites* spp.

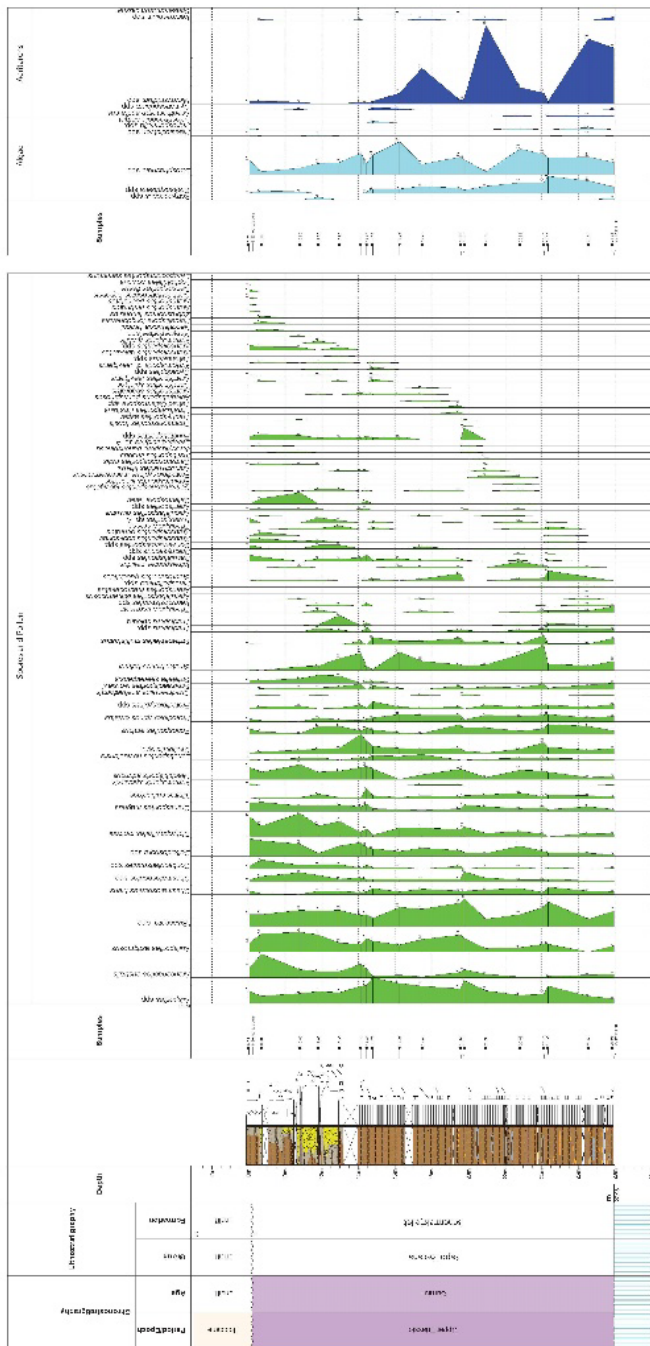
## Appendix II: Table of Re-Os datings from cores 7831/2-U-2 and U-1

Table A1: The radiometric datings by Xu et al. (2014) from cores 7831/2-U-2 and 7831/2-U-1. Included are the uncertainties of the isochron ages and their results after Bayesian data analysis (modified from Xu et al., 2014).

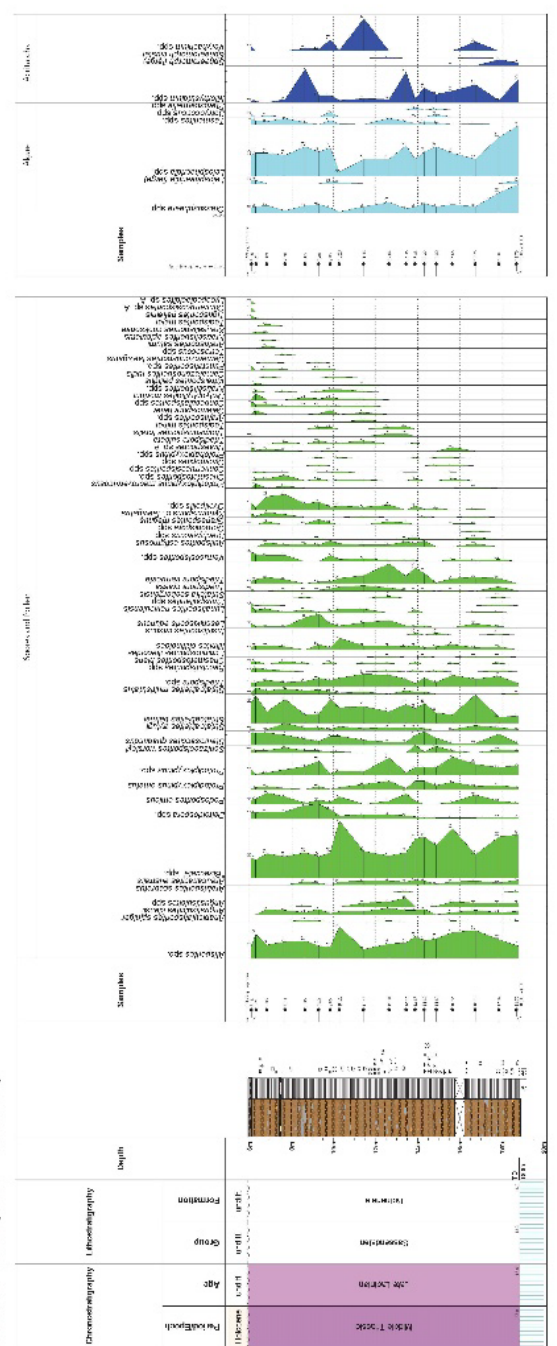
Sampled intervals	Original isochron ages		Results after Bayesian analysis	
	Age (Ma)	2 $\sigma$ (Ma)	Age (Ma)	2 $\sigma$ (Ma)
Core 7831/2-U-1 19.13-19.40 meter	232.0	11.0	231.8	+ 4.8 - 10.1
Core 7831/2-U-1 20.46-20.68 meter*	236.5	3.5	236.2	+ 0.67 - 3.00
Core 7831/2-U-2 10.18-10.34 meter*	236.6	0.39	236.6	+ 0.38 - 0.39
Core 7831/2-U-2 11.12-11.30 meter*	237.6	0.59	237.5	+ 0.56 - 0.59
Core 7831/2-U-2 18.18-18.32 meter	238.4	1.47	238.4	+ 1.26 - 0.90

\* Samples yielding the isochron ages constraining the Ladinian – Carnian boundary.

# Appendix III – Range charts



7831/2-U-2 (5.93 - 18.85m)



## Appendix IV – Plates

Plates of selected palynomorphs recorded from cores 7831/2-U-2 and 7831/2-U-1. If not noted, the photographs are from core 7831/2-U-1. The taxon names are followed by sample depth and England Finder coordinates. The samples were analysed with the label to the right.

### Plate 1

1. *Leschikisporis aduncus* 14.14m, C48-3
2. *Dictyophyllidites mortoni* 14.45m, M60-2
3. *Deltoidospora* sp. 10.82m, U55-2
4. *Calamospora tener* 10.82m, C39
5. *Velosporites* sp. 8.05m, N55-4
6. *Aratrisporites fischeri* 10.82m, D37-3
7. *Aratrisporites macrocavatus* 10.82m, M49

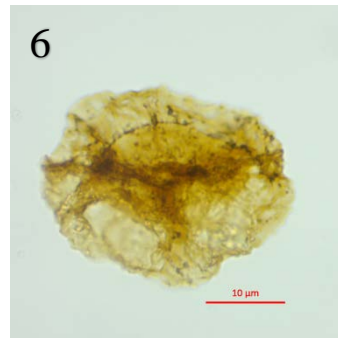
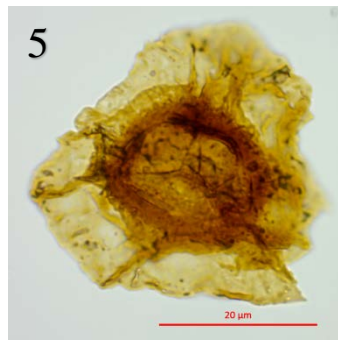
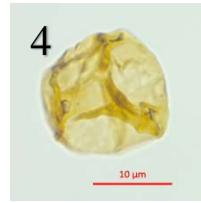
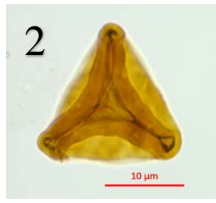
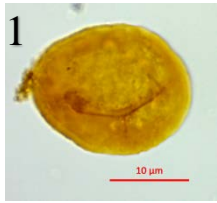


Plate 1

Plate 2

1. *Camarozonosporites rudis* 14.14m, F43
2. *Striatella parva* 10.82m, F40
3. *Striatella seebergensis* 8.05m, T44
4. *Striatella seebergensis* 8.05m, J37
5. *Densosporites fissus* 8.7m, V51-2
6. *Porcellispora longdonensis* 10.82m, E39-2
7. *Apiculatisporites hirsutus* 22.83m, G39-2



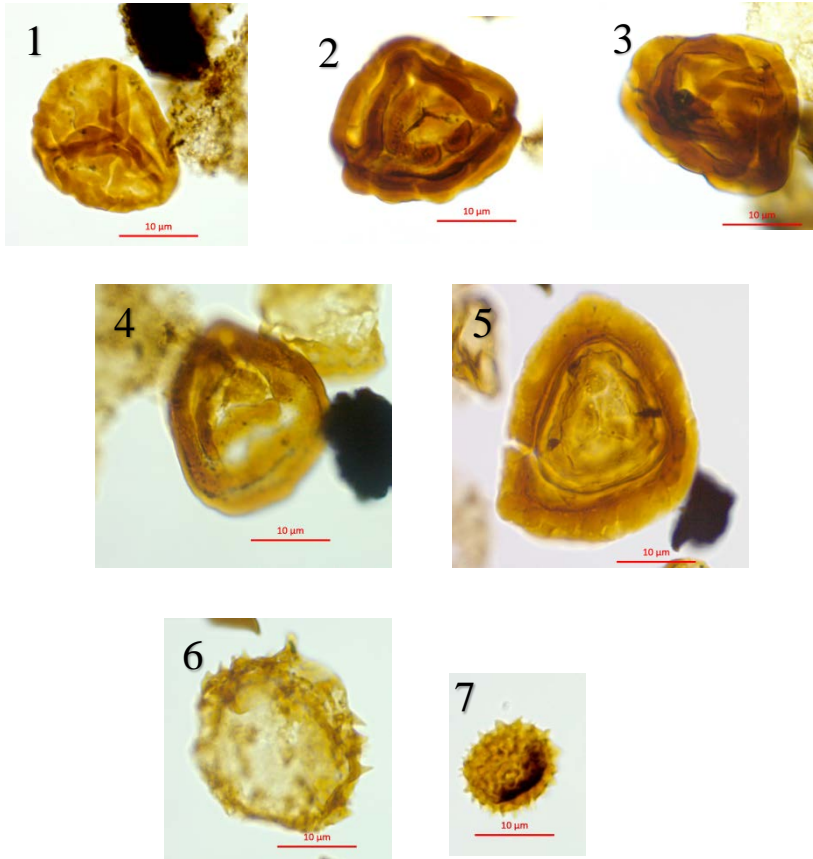


Plate 2

Plate 3

1. *Triadispora verrucata* 10.82m, V36-4
2. *Alisporites* sp. 12.98m, E53-4
3. *Striatoabieites aytugii* 10.82m, N38-3
4. *Striatoabieites balmei* 10.82m, Q64-3
5. *Striatoabieites multistriatus* 14.78m, T59
6. *Lunatisporites noviaulensis* 14.78m, R44
7. *Schizaeoisporites worsleyi* 14.78m, U57-4
8. *Ovalipollis* sp. 14.14m, U38-2
9. *Ovalipollis* sp. 8.05m, U34-1
10. *Staurosaccites quadrifidus* 10.82m, M42

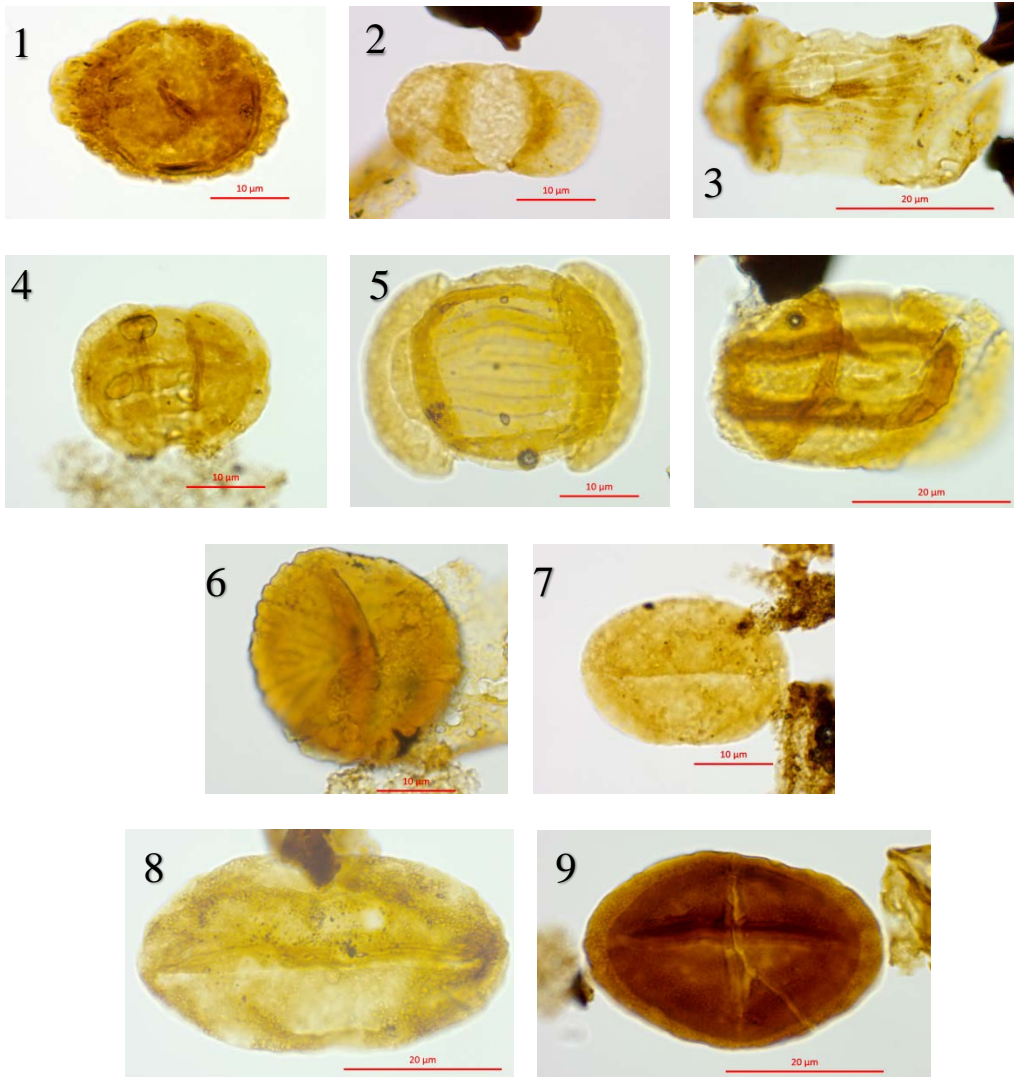


Plate 3

Plate 4

1. *Illinites chitonoides* 10.82m, P53-3
2. *Protodiploxypinus ornatus* 14.14m, Q50-4
3. *Protodiploxypinus macroverrucosus* 20.95m, Q54
4. *Institsporites crispus* 14.14m, G34-2
5. *Aulisporites astigmosus* 22.83m, J43
6. *Aulisporites astigmosus* 10.82m, W53
7. *Podosporites amicus* 10.82m, T54
8. *Granasporites magnus* 14.87m, K56-3
9. *Granasporites magnus* 14.45m D46-4

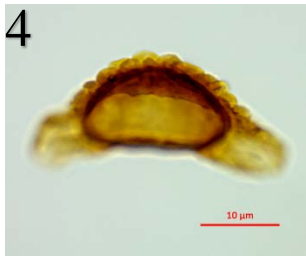
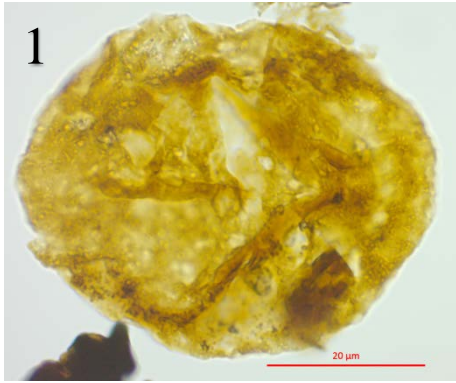


Plate 4

Plate 5

1. *Triadispora* sp. 10.82m, H47-1
2. *Angustisulcites klausii* 14.45m, F54-2
3. *Araucariacites australis* 14.78m, U52
4. *Cycadopites* sp. 10.82m, C47-4
5. *Chasmatosporites hians* 14.45m, E56
6. *Chasmatosporites* sp. 14.78m, S60
7. *Echinosporites iliacoides* 22.83m, H51-2
8. *Echinosporites iliacoides* 16.75m (core 7831/2-U-2), L48-3

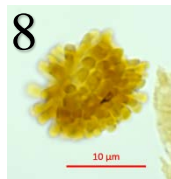
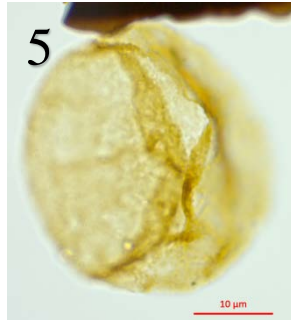
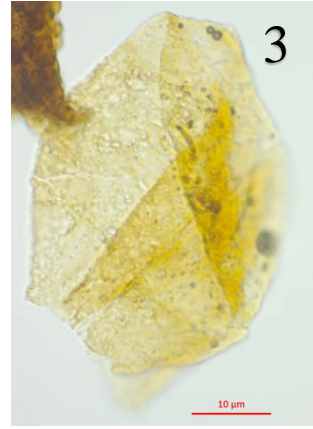
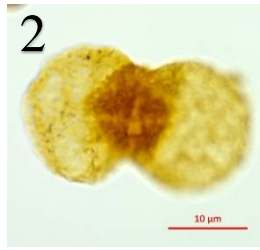


Plate 5

Plate 6

1. *Leiosphaeridia* sp. 14.78m, E56-3
2. *Tasmanites* sp. 26.56m, L45-1
3. *Crassosphaera* sp. 14.78m, N57-1
4. *Pterospermella* sp. 26.56m, N59-3
5. *Botryococcus* sp. 11.82m, R48-2
6. *Micrhystridium* spp. 20.95m, N52
7. *Veryhachium* sp. 14.14m, K35-4
8. Acanthomorph acritarch 24.33m, D61-1



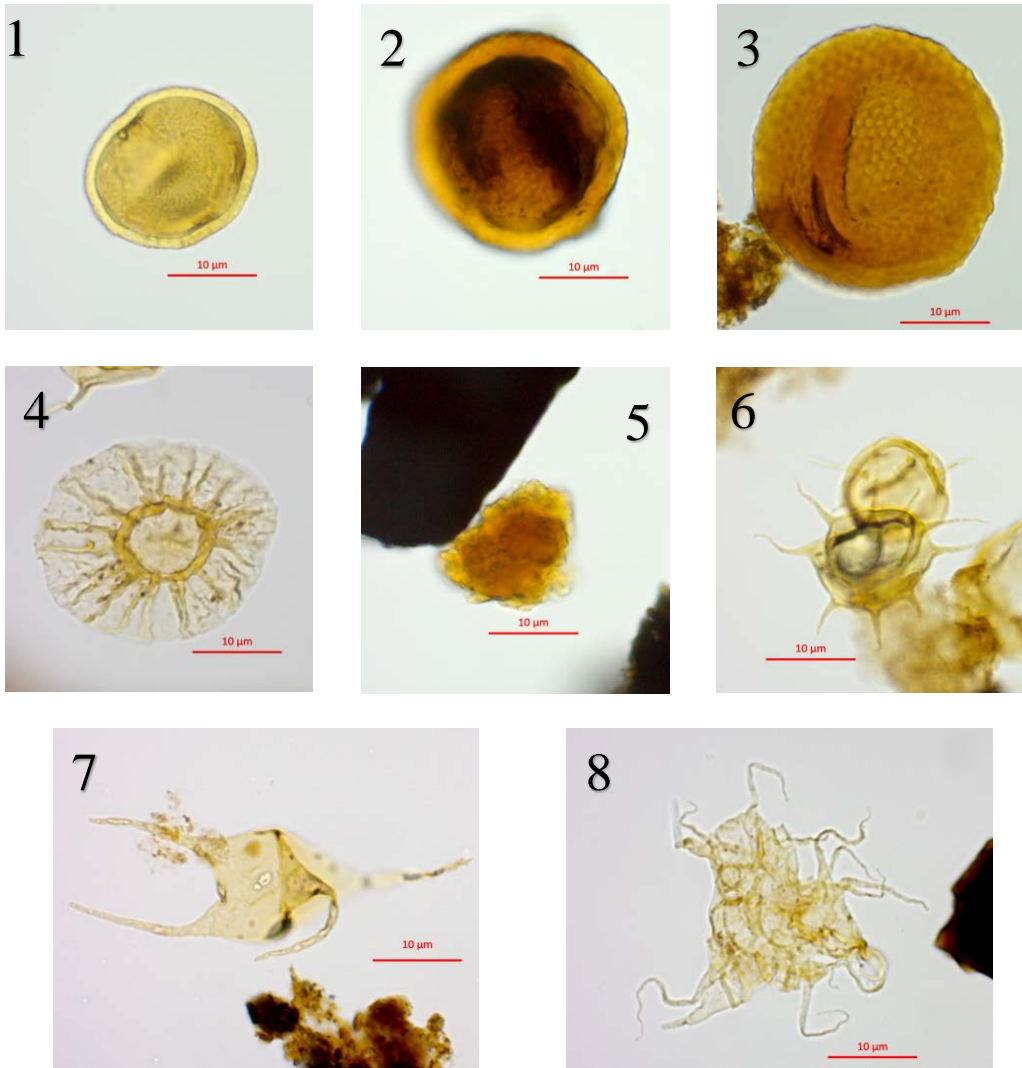


Plate 6